Discover Oncology

ANALYSIS Open Access

Mechanistic role of miR-375 in regulating PDPK1 to promote progression of small bowel neuroendocrine tumors: a silico analysis

Tao Ren[1], Lu Zhou[1], Zhenlong Li[1], Mingmei Pan[1] and Xueqiong Han[2*]

*Correspondence:
Xueqiong Han
hanxueqiong@stu.gxmu.edu.cn
[1]Department of Oncology, The Fifth Affiliated Hospital of Guangxi Medical University, Nanning 530022, Guangxi, China
[2]Department of Oncology, The First Affiliated Hospital Of Guangxi University Of Chinese Medicine, Nanning 530023, Guangxi, China

Abstract

Background The incidence of small bowel neuroendocrine tumors (SBNETs) is steadily increasing, new therapies are urgently needed to prolong the overall survival of patients.

Objective This study aimed to identify diagnostic and therapeutic candidate markers for SBNETs.

Methods Expression profiles of miRNAs were collected from GSE70534, and GSE103317, that of mRNAs were collected from GSE65286. Differentially expressed genes (DEmiRs, DEmRs) were analyzed between SBNETs and controls. Enrichment and coexpression analyses were carried out for DEmRs. XGBoost algorithm was used to screening feature miRNAs. Module genes in SBNETs-related pathways were selected to construct regulated network for feature miRNAs. Drug targeting prediction and immune environment evaluation were identified.

Results A total of 57 common DEmiRs with the same direction of expression were identified. Hsa – miR – 375, hsa – miR – 107, hsa – miR – 1180, hsa – miR – 330 – 3p, and hsa – miR – 328 were identified as feature miRNAs. Among the target genes of feature miRNAs, PDPK1 was the correlation between PDPK1 and the target of Lutetium-177 (177Lu)-DOTATATE was the largest, which were regulated by miR – 375. Additionally, PDPK1 showed correlations with eosinophils, cytotoxic cells, and checkpoints in SBNETs.

Conclusions Five feature miRNAs may have a good diagnostic role for the SBNETs. MiR – 375 regulated PDPK1 may serve as an effective therapeutic candidate marker for SBNETs.

Keywords Small bowel neuroendocrine tumors, PDPK1, miR – 375, 177Lu-DOTATATE

1 Introduction

Neuroendocrine tumors (NETs) originate from a system of neuroendocrine cells in the bronchi and gastrointestinal tract and are highly heterogeneous [1]. NETs can be localized in multiple tissues, such as lung, pancreas, stomach, small intestine, colon [2]. Small bowel neuroendocrine tumors (SBNETs) are epithelial tumors of the small intestine

characterized by neuroendocrine differentiation and the ability to secrete functional hormones or amines [3]. SBNETs account for approximately 17% of all diagnosed nets, with a median overall survival (OS) of 103 months and 5-year survival of 69%, and OS rates decrease with disease extent [4]. Although SBNETs are very small and low proliferative, they have a high propensity to metastasize [5]. At diagnosis, liver metastases are present in approximately 50% of patients and mesenteric lymph node metastases are present in more than 80% of patients [6].

Although considered rare, the incidence and prevalence of SBNETs have been increasing [7]. Surgery plays the most important role in SBNETs treatment and, in principle, can significantly prolong survival and improve patient quality of life [8]. Since most patients are already metastatic at the time of diagnosis or subsequently develop metastases, patients are rarely cured by surgery [9]. Therefore, there is a need to find new potential therapeutic targets in order to implement individualized treatment and improve prognosis.

The molecular basis of SBNETs is not well understood and is difficult to diagnose early in the disease. MicroRNAs (miRNAs) can regulate cell proliferation, differentiation and apoptosis, and their specific roles in cancer can be as oncogenes or tumor suppressors [10]. MiRNAs can be used as a potential prognostic marker for cancer, such as hepatocellular carcinoma [11] and breast cancer [12]. Newly discovered biomarkers such as miRNAs have shown the potential to improve diagnostic SBNETs, even as targets for tumor directed therapy [13]. MiR-1246, miR-1290 and miR-320 as independent prognostic predictors in metastatic neuroendocrine carcinoma patients based second-line treatment, with high expression levels significantly associated with survival, while the effective solution is still uncertain [14]. These findings highlight the potential of miRNAs as valuable tools for understanding tumor biology and improving clinical outcomes. However, little is known about differential miRNA profiles in SBNETs patients.

On the other hand, 3-phosphoinositide-dependent protein kinase-1 (PDPK1) encoded PDK1 kinase, which can activate multiple targets, including Akt [15]. PDPK1 is overexpressed in prostate cancer [16], breast cancer [17], gastric cancer [18], hepatocellular carcinoma [19], and is an essential kinase critical for cell proliferation and viability. In addition, PDPK1 may support hepatocellular cancer metastasis compared to primary tumors [20]. Until now, relatively few studies have evaluated immune cells and checkpoints in SBNETs.

In this study, we explored the differential expression of miRNAs in SBNETs, as well as the underlying regulatory mechanisms. To further identify potential biomarkers and therapeutic targets, as well as associations with the immune microenvironment.

2 Materials and methods

2.1 Data collection and processing

GSE70534, GSE103317, and GSE65286 datasets were collected from gene expression omnibus (GEO) database. GSE70534 [21] included miRNA expression profiles of 28 tumors samples from SBNET patients and 14 adjacent normal small bowel samples based on GPL17537 platform. GSE103317 included miRNA expression profiles of 19 tumors from SBNET patients and 6 normal small intestine mucosa samples based on GPL10406 platform. GSE65286 [22] included mRNA expression profiles of tumor

biopsies from SBNET patients and 10 normal small intestine mucosa samples based on GPL4133 platform. GSE70534 as training set and GSE103317 as a validation set.

Furthermore, the GSE103317 was normalized by the normalizedBetweenArrays function of the limma R package [23]. GSE70534 and GSE65286 were normalized using varianceStabilizingTransformation function from DESeq2 package.

2.2 Differential expression and enrichment analysis

Differentially expressed genes (DEmiRs and DEmRs) between SBNET and controls were analyzed using limma R package [23] in all three datasets. DEmiRs with same direction of expression in GSE70534, and GSE103317 were considered as common DEmiRs. An adjusted $P < 0.05$ was used as screening threshold.

Enrichment analysis of Gene Ontology (GO) and Kyoto Encyclopedia of Genes and Genomes (KEGG) pathways for DEmRs was performed using clusterProfiler R package [24]. A $P < 0.05$ were considered as significant. Gene set enrichment analysis (GSEA) was also carried out using GSEA software.

2.3 Construction of diagnostic model

Diagnostic models were constructed for common DEmiRs using the XGBoost R package [25]. A training set (GSE70534) and a validation set (GSE103317) were used for eXtreme Gradient Boosting (XGBoost) algorithm. Then, the importance score of a feature can be obtained based on its involvement in utilizing the augmented decision tree for critical decisions. All features are ranked in descending order according to their importance score, with higher scores indicating that the feature is more important. For this, Shapley values were used, which is a concept recently taken from cooperative game theory and applied to machine learning [26].

2.4 Weighted gene co-expression network analysis

Weighted gene co-expression network analysis (WGCNA) was performed to construct coexpression network of DEmRs. In brief, we selected appropriate soft threshold parameters to ensure network obeyed scale-free criteria through the WGCNA algorithm [27]. Then adjacency matrix was created using the topological overlap measure (TOM). Genes with similar expression patterns were clustered into the same gene modules. The criteria of minModuleSize of 30, and mergeCutHeight of 0.25 were defined. Finally, the WGCNA modules were identified.

2.5 Receiver operation characteristic (ROC) analysis

According to ROC analysis of GSE70534 area under the ROC (AUC) values of the feature miRNAs were assessed using the pROC R package. The higher the AUC value, the better the diagnostic efficacy.

2.6 MiRNA regulation network

The ceRNA network is constructed based on the interaction relationships between lncRNA, circRNA, miRNA, and mRNA. It is worth noting that the ceRNA hypothesis indicates that its expression level should be negatively correlated with miRNA expression and positively correlated with mRNA expression [28]. Therefore, we identified the mRNA regulated by feature miRNAs were searched for further analysis. The mRNAs

targeted by the feature miRNAs were collected in the Targetscan database (https://www.targetscan.org/vert_80/), DEmRNAs of GSE65286 targeted by the feature miRNAs, then matching pathway genes related to disease. Among there, expression of feature miRNAs and mRNAs were opposite. Finally, the target genes were further screened by intersected with WGCNA module genes and SBNET-related pathway genes.

2.7 Drug targeting prediction

NETs-related therapeutic drugs were obtained from Drugbank database (https://go.drugbank.com/). Correlation of target genes of miRNAs and 5 target genes of drugs were calculated using Pearson correlation analysis.

The SSTR1 protein structure was downloaded from the UniProt database (https://www.uniprot.org/) and saving as a PDB format file. It was subsequently imported into sybylx-2.1 software for preprocessing, including removal of water molecules, and hydrogenation. The SDF file of 3D structure of drug was downloaded from PubChem database for energy optimization using Chem3D 20.0 software. The corresponding compounds were docked with the protein using the Surflex-Dock module in sybylx-2.1 software and evaluated using the scoring function. Docking results were presented with PyMOL. 2.5.2 software.

2.8 Immune cell infiltration

The single-sample GSEA (ssGSEA) was performed to quantify the score of gene markers of immune cells using GSVA R software package [29]. Difference scores between SBNET and controls were assessed using limma R package. Expression of checkpoints was detected in SBNET and controls were also assessed using limma R package. Correlations between key gene and immune cells or checkpoints were determined using Pearson correlation analysis.

2.9 Statistical methods

All the analyses of the study were constructed by Bioinforcloud platform (https://www.bioinforcloud.org.cn).

3 Results

3.1 Identification of feature MiRNAs

Overview design of this study is shown in Fig. 1. To identify miRNAs that are aberrantly expressed in SBNET, we performed differential analysis. In GSE70534 dataset, we obtained 351 DEmiRs (Fig. 2A), in GSE103317 dataset, we obtained 262 DEmiRs (Fig. 2B). Then a total of 57 common DEmiRs were identified (Fig. 2C), with 38 up-regulated and 19 down-regulated expression in SBNET. Diagnostic models were constructed using XGBoost algorithm for common DEmiRs in the GSE70534 dataset. The model was validated with good diagnostic efficacy in the GSE103317 dataset (Fig. 2D). The importance of features ranking with SHAP values for the XGBoost model, the top five most important variables is presented in Fig. 2E. Including hsa – miR – 375, hsa – miR – 107, hsa – miR – 1180, hsa – miR – 330 – 3p, and hsa – miR – 328. Figure 2F showed the interaction effect of feature DEmiRs and their corresponding SHAP value.

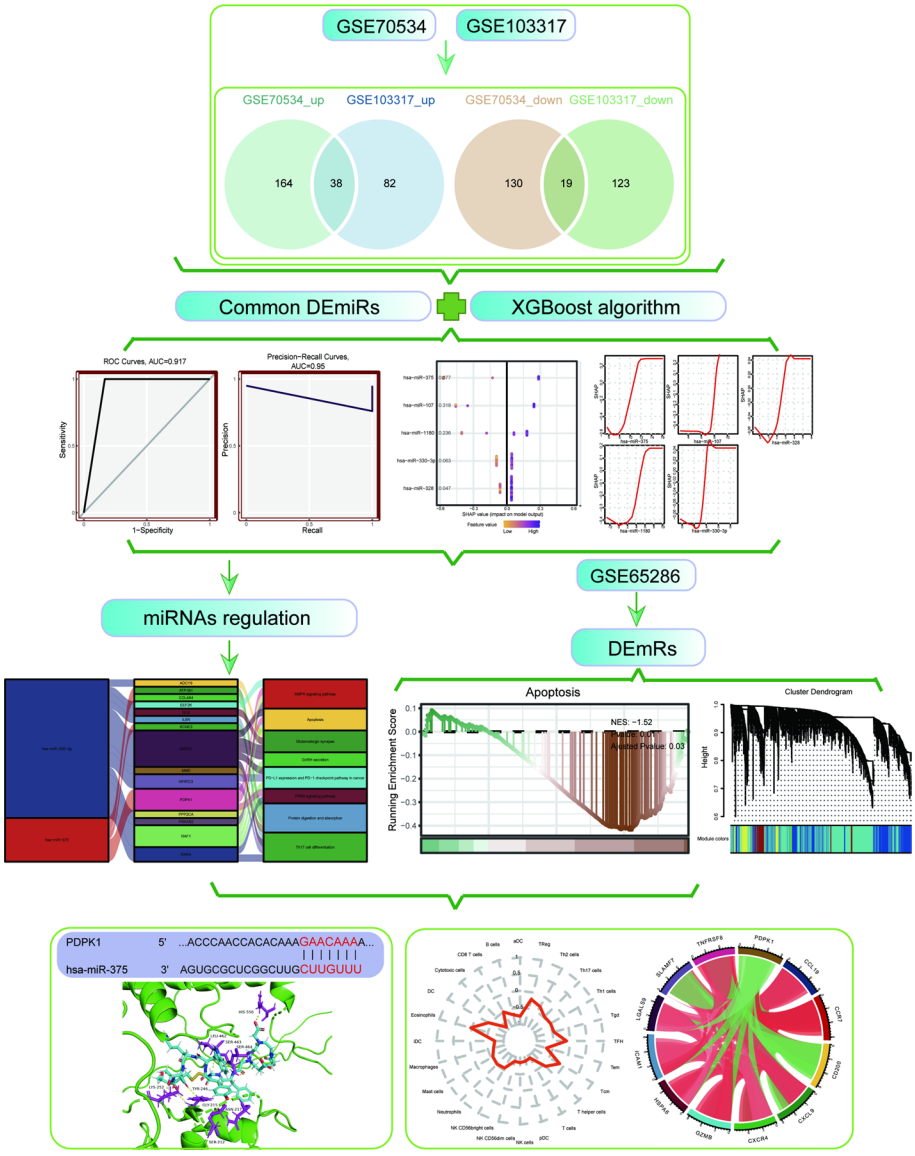

Fig. 1 The flowchart of this study. *AUC* area under the receiver operation characteristic curve; Differentially expressed mRNAs, *DEmRs* Differentially expressed miRNAs, *DEmiRs* ROC, receiver operation characteristic curve; *XGBoost* eXtreme Gradient Boosting

3.2 Biological functions and coexpression networks

Firstly, we found 8606 DEmRs in GSE65286 dataset (Fig. 3A). In the GO enrichment results, we found that small molecule catabolic process, fatty acid metabolic process, and alcohol metabolic process were mainly enriched by DEmRs (Fig. 3B). Additionally, we found that MAPK signaling pathway, carbon metabolism, and apoptosis were involved in DEmRs (Fig. 3C).

On the other hand, we constructed coexpression network for DEmRs. The soft threshold was selected as 18 to construct coexpression network (Fig. 3D). We then identified 5 meaningful modules and 8551 module genes (Fig. 3E).

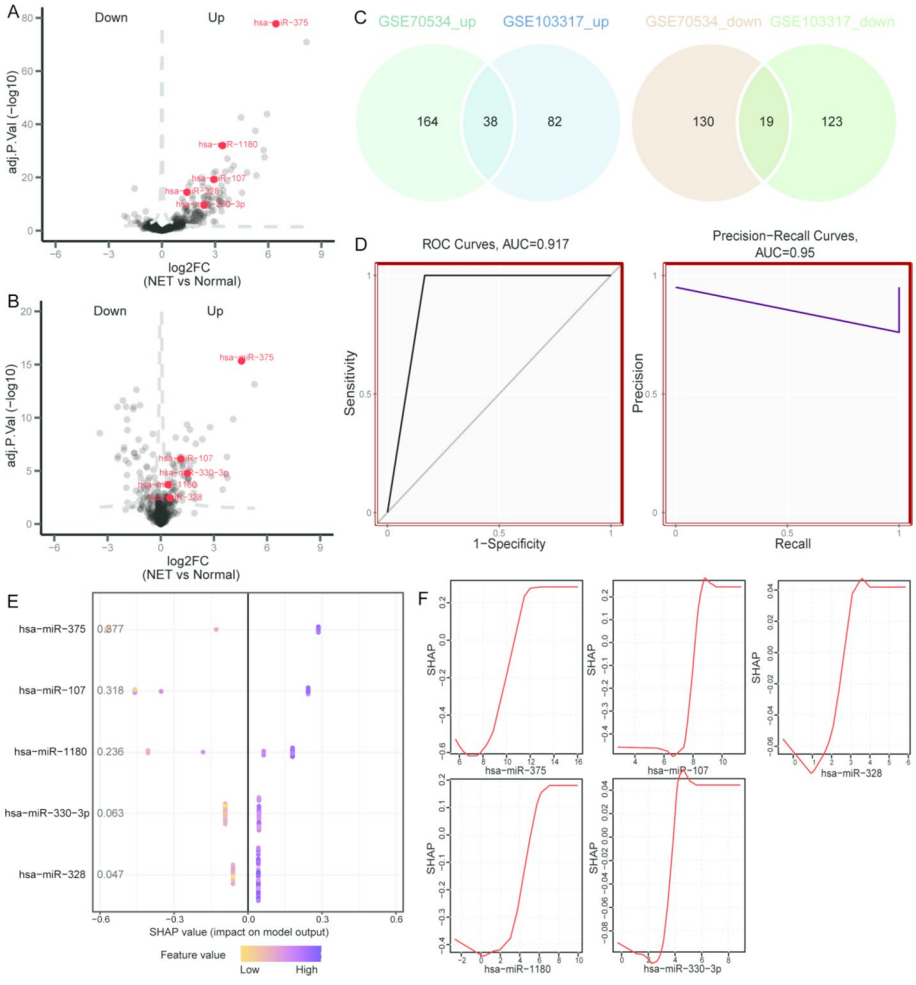

Fig. 2 Construction of diagnostic model and identification of feature miRNAs. **A** Volcano plot of differentially expressed miRNAs between SBNET and controls in GSE70534 dataset. **B** Volcano plot of differentially expressed miRNAs between SBNET and controls in GSE103317 dataset. **C** Intersection of up-regulated or down-regulated miRNAs in GSE70534 and GSE103317 datasets were considered as common DEmiRs. **D** The receiver operation characteristic (ROC) curves and precision-recall curves of XGBoost algorithm in GSE103317 dataset. **E** The attributes of top five features in the XGBoost model. SHAP, SHapley additive explanation. **F** SHAP values interacted with five features

3.3 Targets prediction of feature MiRNAs

To identify the targets of five feature miRNAs, we first observed the expression levels in SBNET and controls (Fig. 4A and B). Interestingly, these miRNAs were all highly expressed in SBNET. The AUC values of five feature miRNAs were all than 0.96, indicating that they all had high diagnostic efficacy (Fig. 4C). In the results of GSEA, we found AMPK signaling pathway, Apoptosis, Th17 cell differentiation, PPAR signaling pathway, PD-L1 expression and PD-1 checkpoint pathway in cancer, GnRH secretion, Glutamatergic synapse, Protein digestion and absorption also appeared in the KEGG enrichment results, and considered as SBNET-related pathways (Fig. 5). By matching the genes in SBNET-related pathways, we finally obtained the target genes of feature miRNAs. And Hsa – miR – 375, and hsa – miR – 330 – 3p targeted 15 module genes and involved SBNET-related pathways (Fig. 4D; Table 1).

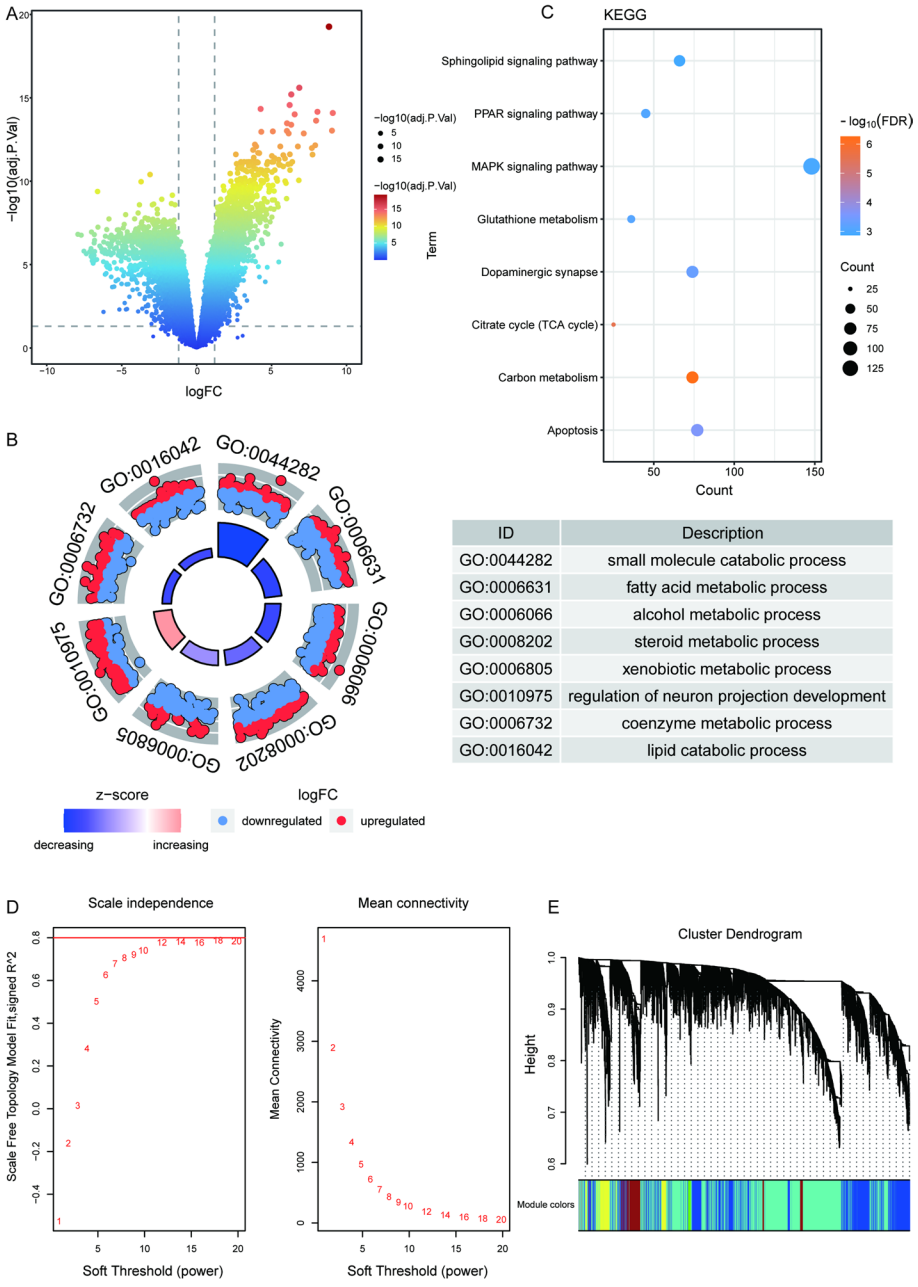

ID	Description
GO:0044282	small molecule catabolic process
GO:0006631	fatty acid metabolic process
GO:0006066	alcohol metabolic process
GO:0008202	steroid metabolic process
GO:0006805	xenobiotic metabolic process
GO:0010975	regulation of neuron projection development
GO:0006732	coenzyme metabolic process
GO:0016042	lipid catabolic process

Fig. 3 Biological functions and coexpression network of DEmRs. **A** Volcano plot of differentially expressed mRNAs between SBNET and controls in GSE65286 dataset. **B** Mainly biological processes of DEmRs involved. **C** Kyoto Encyclopedia of Genes and Genomes pathways of DEmRs involved. **D** Appropriate soft threshold parameters selection in WGCNA. **E** Dendrogram of coexpression network modules

3.4 Drug prediction and immune scoring in SBNET

Online prediction results found 177Lu-DOTATATE could be targeted to treat the gastroenteropancreatic neuroendocrine tumors. The target genes of 177Lu-DOTATATE were omatostatin receptors (SSTRs), a family of G protein coupled receptors. Correlation results showed that PDPK1 and SSTR1 were most highly correlated, and being identified as key gene (Fig. 6A). Figure 6B showed the binding sites between PDPK1 and miR – 375. Docking score of SSTR1 and 177Lu-DOTATATE (Fig. 6C) was 11.77, which against the active sites of SSTR1 (Fig. 6D).

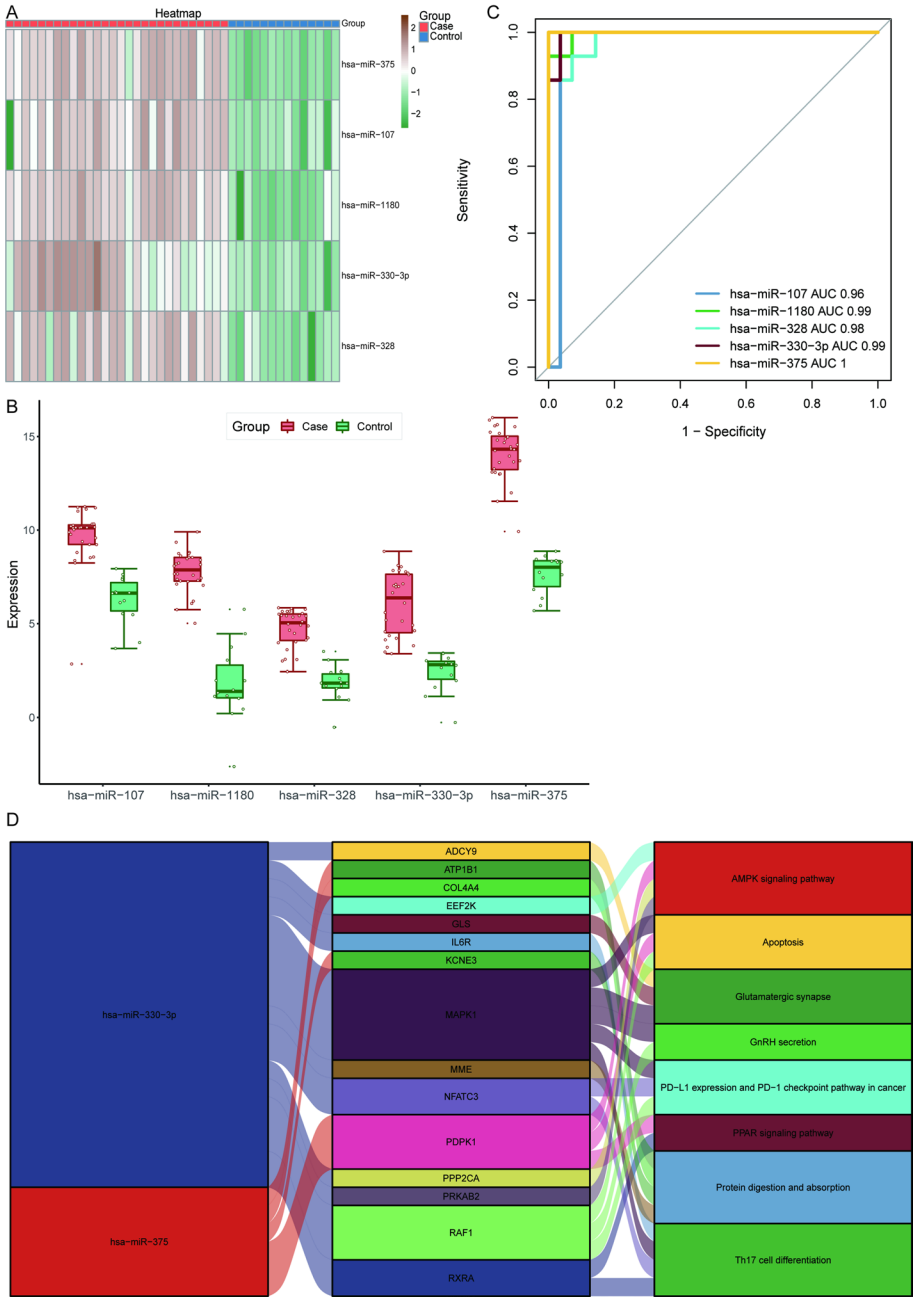

Fig. 4 Diagnostic power of five feature miRNAs and prediction of their target genes. Heatmap **A** and box plots **B** of feature miRNAs expression in SBNET and controls in GSE70534 dataset. **C** ROC curves of five feature miRNAs. AUC, area under the receiver operation characteristic curve. **D** Regulatory networks of feature miRNAs and target genes, as well as involved pathways

In addition, we also assessed the levels of immune cells in SBNET (Fig. 6E). Significantly elevated pDC cells are found in disease, whereas B cells are significantly decreased. Correlation results showed that PDPK1 was significantly positively correlated with eosinophils and negatively correlated with cytotoxic cells (Fig. 6F). Additionally, PDPK1 was significantly positively correlated with CD200 and negatively correlated with CCR7 (Fig. 7A). Interestingly, CD200 was upregulated and CCR7 is downregulated in SBNET (Fig. 7B). This study reveals the therapeutic potential of 177Lu-DOTATATE

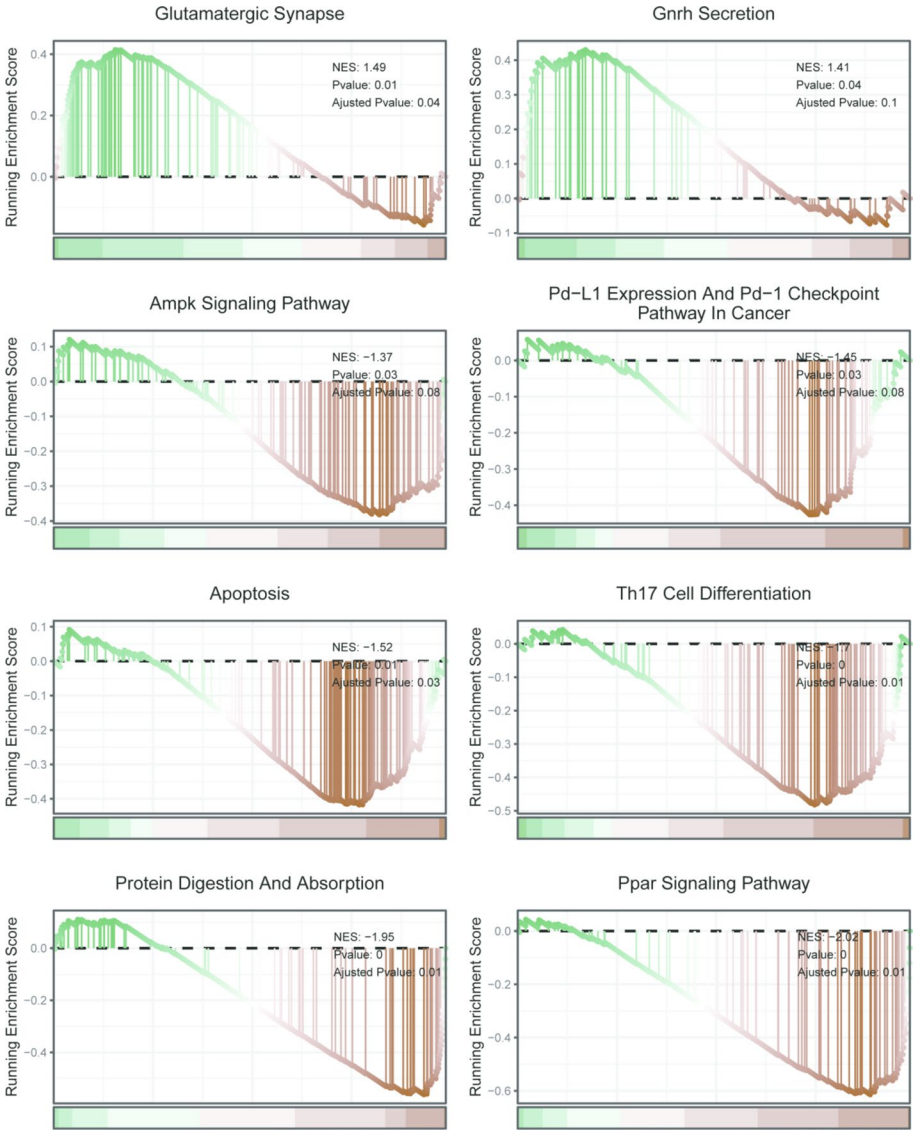

Fig. 5 Intersected Kyoto Encyclopedia of Genes and Genomes pathways between enrichment analysis and gene set enrichment analysis results

in gastroenteropancreatic neuroendocrine tumors through targeting of somatostatin receptor SSTR1 and modulation of the PDPK1-miR-375 axis. Additionally, we observed a significant increase in pDCs and a decrease in B cells within SBNETs. PDPK1 exhibited positive correlations with eosinophils but negative correlations with cytotoxic cells and CCR7, suggesting its role in driving disease progression via an immunosuppressive tumor microenvironment.

4 Discussion

In this study, on the basis of comparing miRNA profiles between SBNETs and controls, we utilized the XGBoost algorithm to build a diagnostic model and identified signature miRNAs. We further found that high expression of these miRNAs had a high predictive probability for the diagnosis of SBNETs. In addition, we constructed a coexpression network for the differentially expressed mRNAs, and identified the target genes of feature

Table 1 mRNAs targeted by the feature MicroRNAs were collected in the targetscan database

miRNA	Target mRNA	miRNA	Target mRNA	miRNA	Target mRNA
hsa-miR-107	NEK10	hsa-miR-328-3p	EIF4EBP1	hsa-miR-1180-3p	CCDC3
hsa-miR-107	AGFG1	hsa-miR-328-3p	PGM2	hsa-miR-1180-3p	SH2D4A
hsa-miR-107	RRAGC	hsa-miR-328-3p	DNAJC4	hsa-miR-1180-3p	ITGA6
hsa-miR-107	AMMECR1	hsa-miR-328-3p	FOXS1	hsa-miR-1180-3p	ARNT2
hsa-miR-107	MLK4	hsa-miR-328-3p	CTNNBIP1	hsa-miR-1180-3p	KANSL3
hsa-miR-107	SNX18	hsa-miR-328-3p	CHP2	hsa-miR-1180-3p	ARAP1
hsa-miR-107	ZBTB39	hsa-miR-328-3p	DUSP16	hsa-miR-1180-3p	AMZ1
hsa-miR-107	GPR6	hsa-miR-328-3p	CHST7	hsa-miR-1180-3p	AGBL4
hsa-miR-107	STAMBPL1	hsa-miR-328-3p	TCF7L2	hsa-miR-1180-3p	DHX33
hsa-miR-107	PCDH17	hsa-miR-328-3p	KLHL42	hsa-miR-1180-3p	CASP9
hsa-miR-107	TNRC6B	hsa-miR-328-3p	EDARADD	hsa-miR-1180-3p	ZNF618
hsa-miR-107	IGSF3	hsa-miR-328-3p	LYVE1	hsa-miR-1180-3p	SEPT11
hsa-miR-107	HMGB1	hsa-miR-328-3p	FUBP1	hsa-miR-1180-3p	PPP1R3B
hsa-miR-107	AP3M1	hsa-miR-328-3p	UBFD1	hsa-miR-1180-3p	ZNF585A
hsa-miR-107	CLCN5	hsa-miR-328-3p	NF2	hsa-miR-1180-3p	HAUS3
hsa-miR-107	ACACB	hsa-miR-328-3p	NXPH3	hsa-miR-1180-3p	SEMA4F
hsa-miR-107	USP14	hsa-miR-328-3p	SNX21	hsa-miR-1180-3p	CTDSP2
hsa-miR-107	KB-1507C5.2	hsa-miR-328-3p	DYNC1I1	hsa-miR-1180-3p	MSI1
hsa-miR-107	AGO3	hsa-miR-328-3p	TMEM229A	hsa-miR-1180-3p	CEP72
hsa-miR-107	MTMR3	hsa-miR-328-3p	TESK2	hsa-miR-1180-3p	DNASE1L1
hsa-miR-1180-3p	RPS19BP1	hsa-miR-328-3p	NR3C1	hsa-miR-1180-3p	PLXNB2
hsa-miR-1180-3p	SAG	hsa-miR-328-3p	CHTF8	hsa-miR-1180-3p	ZNF605
hsa-miR-1180-3p	ISG15	hsa-miR-328-3p	RGL2	hsa-miR-1180-3p	GPR173
hsa-miR-1180-3p	PPP1R17	hsa-miR-328-3p	PIGA	hsa-miR-1180-3p	PHF14
hsa-miR-1180-3p	HFM1	hsa-miR-328-3p	NPFFR1	hsa-miR-1180-3p	PIGL
hsa-miR-1180-3p	GGACT	hsa-miR-328-3p	NOTCH2NL	hsa-miR-1180-3p	C19orf48
hsa-miR-1180-3p	C19orf68	hsa-miR-328-3p	RANBP10	hsa-miR-1180-3p	BCR
hsa-miR-1180-3p	KAAG1	hsa-miR-328-3p	SLC2A1	hsa-miR-1180-3p	FOXK1
hsa-miR-1180-3p	CMTM7	hsa-miR-328-3p	FAM214B	hsa-miR-1180-3p	C11orf88
hsa-miR-1180-3p	PHLDB3	hsa-miR-328-3p	RWDD2B	hsa-miR-1180-3p	AP4S1
hsa-miR-1180-3p	KANSL1	hsa-miR-328-3p	FAXDC2	hsa-miR-1180-3p	SYNM
hsa-miR-1180-3p	TMEM92	hsa-miR-328-3p	SRSF9	hsa-miR-1180-3p	THSD4
hsa-miR-1180-3p	ZNF83	hsa-miR-328-3p	ULK2	hsa-miR-1180-3p	TBC1D5
hsa-miR-1180-3p	PRDM7	hsa-miR-328-3p	ITGA5	hsa-miR-1180-3p	ANO6
hsa-miR-1180-3p	C9orf47	hsa-miR-328-3p	C16orf87	hsa-miR-1180-3p	DUSP22
hsa-miR-1180-3p	KLF14	hsa-miR-328-3p	EN2	hsa-miR-1180-3p	NKX2-4
hsa-miR-1180-3p	AKR1C2	hsa-miR-328-3p	PARP16	hsa-miR-1180-3p	ASXL3
hsa-miR-1180-3p	COL23A1	hsa-miR-328-3p	MAN1C1	hsa-miR-1180-3p	BTBD19
hsa-miR-1180-3p	PRR23C	hsa-miR-328-3p	MMP16	hsa-miR-1180-3p	CNTN4
hsa-miR-1180-3p	HPCAL4	hsa-miR-328-3p	ADNP	hsa-miR-1180-3p	LRRC14
hsa-miR-1180-3p	SCRT2	hsa-miR-328-3p	TRAPPC6B	hsa-miR-1180-3p	SMG6
hsa-miR-1180-3p	PRIMA1	hsa-miR-328-3p	DDI2	hsa-miR-1180-3p	ABCC12
hsa-miR-1180-3p	C6orf120	hsa-miR-328-3p	PSME3	hsa-miR-1180-3p	CCDC127
hsa-miR-1180-3p	IGDCC3	hsa-miR-328-3p	GBA	hsa-miR-1180-3p	C1orf21
hsa-miR-1180-3p	RNF5	hsa-miR-328-3p	DERL2	hsa-miR-1180-3p	SLC25A15
hsa-miR-1180-3p	RP4-758J18.2	hsa-miR-328-3p	HPCAL4	hsa-miR-1180-3p	ABHD17A
hsa-miR-1180-3p	C17orf74	hsa-miR-328-3p	SHISA5	hsa-miR-1180-3p	USP6NL
hsa-miR-1180-3p	TMIE	hsa-miR-328-3p	PODNL1	hsa-miR-1180-3p	ZBED1
hsa-miR-1180-3p	PPP2R5E	hsa-miR-328-3p	PIM1	hsa-miR-1180-3p	PLA2G4F
hsa-miR-1180-3p	RUFY1	hsa-miR-328-3p	HIST1H4D	hsa-miR-1180-3p	NDST1
hsa-miR-1180-3p	MKNK2	hsa-miR-328-3p	SLC30A8	hsa-miR-1180-3p	SH3BP4
hsa-miR-1180-3p	RIPPLY1	hsa-miR-328-3p	USP37	hsa-miR-1180-3p	KMT2A
hsa-miR-1180-3p	TEF	hsa-miR-328-3p	KAT6B	hsa-miR-1180-3p	GLI2

Table 1 (continued)

miRNA	Target mRNA	miRNA	Target mRNA	miRNA	Target mRNA
hsa-miR-1180-3p	OTUD7B	hsa-miR-328-3p	LNX2	hsa-miR-1180-3p	ZNF791
hsa-miR-1180-3p	BIN2	hsa-miR-328-3p	MXI1	hsa-miR-1180-3p	FAM83C
hsa-miR-1180-3p	FXYD5	hsa-miR-328-3p	HIST1H4L	hsa-miR-1180-3p	CTBP1
hsa-miR-1180-3p	P4HB	hsa-miR-328-3p	USP8	hsa-miR-1180-3p	MTA3
hsa-miR-1180-3p	ZNF341	hsa-miR-328-3p	EBF4	hsa-miR-1180-3p	SH3RF2
hsa-miR-1180-3p	KCNA6	hsa-miR-328-3p	TP73	hsa-miR-1180-3p	INPPL1
hsa-miR-1180-3p	DNAH11	hsa-miR-328-3p	GBX2	hsa-miR-1180-3p	ADRA1D
hsa-miR-1180-3p	ETS1	hsa-miR-328-3p	MAP3K9	hsa-miR-1180-3p	CCNF
hsa-miR-1180-3p	MAPRE3	hsa-miR-328-3p	CA3	hsa-miR-1180-3p	BAK1
hsa-miR-1180-3p	PRX	hsa-miR-328-3p	FOXO4	hsa-miR-1180-3p	PROB1
hsa-miR-1180-3p	FUOM	hsa-miR-328-3p	C19orf43	hsa-miR-1180-3p	MDM4
hsa-miR-1180-3p	MYO15A	hsa-miR-328-3p	LGR4	hsa-miR-1180-3p	RASA4
hsa-miR-1180-3p	IL17RE	hsa-miR-328-3p	POLR3H	hsa-miR-1180-3p	MAFK
hsa-miR-1180-3p	NKIRAS2	hsa-miR-328-3p	SNRK	hsa-miR-1180-3p	UBE2D4
hsa-miR-1180-3p	TMTC2	hsa-miR-328-3p	HIC1	hsa-miR-1180-3p	OTUD3
hsa-miR-1180-3p	NTRK1	hsa-miR-328-3p	ZNF697	hsa-miR-1180-3p	SERPINH1
hsa-miR-1180-3p	OLFM2	hsa-miR-328-3p	ESCO1	hsa-miR-1180-3p	ZBTB10
hsa-miR-1180-3p	C11orf34	hsa-miR-328-3p	TTC26	hsa-miR-1180-3p	ADH6
hsa-miR-1180-3p	TNIP2	hsa-miR-328-3p	C10orf113	hsa-miR-1180-3p	SCAMP1
hsa-miR-1180-3p	SNRPA	hsa-miR-328-3p	ZNF436	hsa-miR-1180-3p	WNT8B
hsa-miR-1180-3p	TMEM178B	hsa-miR-328-3p	STT3A	hsa-miR-1180-3p	HPCA
hsa-miR-1180-3p	THNSL2	hsa-miR-328-3p	ZNF280B	hsa-miR-1180-3p	SGCD
hsa-miR-1180-3p	CTU2	hsa-miR-328-3p	ARL6IP1	hsa-miR-1180-3p	ARID1B
hsa-miR-1180-3p	SCAMP4	hsa-miR-328-3p	WASF2	hsa-miR-1180-3p	IFFO2
hsa-miR-1180-3p	ZDHHC18	hsa-miR-328-3p	PTPN9	hsa-miR-1180-3p	PPARGC1B
hsa-miR-1180-3p	HPR	hsa-miR-328-3p	NKPD1	hsa-miR-1180-3p	ATP8A2
hsa-miR-1180-3p	C1orf127	hsa-miR-328-3p	NKIRAS2	hsa-miR-1180-3p	HOXB4
hsa-miR-1180-3p	B4GALT7	hsa-miR-328-3p	DNAH10OS	hsa-miR-1180-3p	DGKZ
hsa-miR-1180-3p	MYZAP	hsa-miR-328-3p	SOGA1	hsa-miR-1180-3p	LIN54
hsa-miR-1180-3p	PLXNB3	hsa-miR-328-3p	PEF1	hsa-miR-1180-3p	TMEM201
hsa-miR-1180-3p	VEGFB	hsa-miR-328-3p	RSBN1L	hsa-miR-1180-3p	SPTBN4
hsa-miR-1180-3p	ID3	hsa-miR-328-3p	MPV17	hsa-miR-1180-3p	TRIM9
hsa-miR-1180-3p	AC110619.2	hsa-miR-328-3p	MBNL3	hsa-miR-1180-3p	OTUD6A
hsa-miR-1180-3p	HP	hsa-miR-328-3p	LHFPL2	hsa-miR-1180-3p	TTYH3
hsa-miR-1180-3p	MCF2L2	hsa-miR-328-3p	SLC27A4	hsa-miR-1180-3p	CNTROB
hsa-miR-1180-3p	EIF1	hsa-miR-328-3p	NRIP1	hsa-miR-1180-3p	KIAA1147
hsa-miR-1180-3p	PCID2	hsa-miR-328-3p	KIF2A	hsa-miR-1180-3p	HECW1
hsa-miR-1180-3p	ADAMTS10	hsa-miR-328-3p	ITGA9	hsa-miR-1180-3p	ZNF333
hsa-miR-1180-3p	hsa-mir-1199	hsa-miR-328-3p	ZC3H12B	hsa-miR-1180-3p	FLNB
hsa-miR-1180-3p	CERS1	hsa-miR-328-3p	HIF1AN	hsa-miR-1180-3p	RIMS4
hsa-miR-1180-3p	SLC26A4	hsa-miR-328-3p	METTL21B	hsa-miR-1180-3p	CADM3
hsa-miR-1180-3p	CTRC	hsa-miR-328-3p	ACSS2	hsa-miR-1180-3p	RAD54L2
hsa-miR-1180-3p	WDR1	hsa-miR-328-3p	YWHAZ	hsa-miR-1180-3p	TBC1D28
hsa-miR-1180-3p	C20orf27	hsa-miR-328-3p	PTPRU	hsa-miR-1180-3p	TTLL12
hsa-miR-1180-3p	ZBED2	hsa-miR-328-3p	H2AFX	hsa-miR-1180-3p	CBL
hsa-miR-1180-3p	SUN1	hsa-miR-328-3p	HAP1	hsa-miR-1180-3p	ZNF517
hsa-miR-1180-3p	NCS1	hsa-miR-328-3p	MICALL1	hsa-miR-1180-3p	PLCE1
hsa-miR-1180-3p	STRA6	hsa-miR-328-3p	C6orf223	hsa-miR-1180-3p	SNX29
hsa-miR-1180-3p	TRIM62	hsa-miR-328-3p	PCNXL4	hsa-miR-1180-3p	POU3F3
hsa-miR-1180-3p	CYB561	hsa-miR-328-3p	SHKBP1	hsa-miR-1180-3p	ZNF660
hsa-miR-1180-3p	GLTPD1	hsa-miR-328-3p	FAM199X	hsa-miR-1180-3p	MN1
hsa-miR-1180-3p	SCN5A	hsa-miR-328-3p	SCN2B	hsa-miR-1180-3p	MLEC
hsa-miR-1180-3p	SH3BGRL2	hsa-miR-328-3p	FAM211A	hsa-miR-1180-3p	TRAM2

Table 1 (continued)

miRNA	Target mRNA	miRNA	Target mRNA	miRNA	Target mRNA
hsa-miR-1180-3p	BMF	hsa-miR-328-3p	ANKRD40	hsa-miR-1180-3p	ADAL
hsa-miR-1180-3p	GAPDHS	hsa-miR-328-3p	KIAA0247	hsa-miR-1180-3p	SH3RF1
hsa-miR-1180-3p	RPL18	hsa-miR-328-3p	RNF152	hsa-miR-1180-3p	CEBPD
hsa-miR-1180-3p	FOXP4	hsa-miR-328-3p	SLITRK3	hsa-miR-1180-3p	PRLR
hsa-miR-1180-3p	FOXE1	hsa-miR-328-3p	SLC7A6	hsa-miR-1180-3p	VASN
hsa-miR-1180-3p	BAD	hsa-miR-328-3p	VAMP2	hsa-miR-1180-3p	TBX5
hsa-miR-1180-3p	MED13L	hsa-miR-328-3p	ERMP1	hsa-miR-1180-3p	WDR7
hsa-miR-1180-3p	PDPR	hsa-miR-328-3p	RPS9	hsa-miR-1180-3p	FAM174B
hsa-miR-1180-3p	GLIS1	hsa-miR-328-3p	KIAA1614	hsa-miR-1180-3p	GAN
hsa-miR-1180-3p	ABCC6	hsa-miR-328-3p	CCDC88A	hsa-miR-1180-3p	SNX19
hsa-miR-1180-3p	GPR17	hsa-miR-328-3p	ZNF423	hsa-miR-1180-3p	GALNT6
hsa-miR-1180-3p	TBPL2	hsa-miR-328-3p	TRIM71	hsa-miR-1180-3p	C11orf87
hsa-miR-1180-3p	MPHOSPH8	hsa-miR-328-3p	RPP14	hsa-miR-1180-3p	UBE2J2
hsa-miR-1180-3p	ZSWIM6	hsa-miR-328-3p	PHF15	hsa-miR-1180-3p	KIF13B
hsa-miR-1180-3p	ST3GAL3	hsa-miR-328-3p	RS1	hsa-miR-1180-3p	ZNF276
hsa-miR-1180-3p	XXbac-BPG32J3.20	hsa-miR-328-3p	ESRP1	hsa-miR-1180-3p	TPGS1
hsa-miR-1180-3p	RP11-302B13.5	hsa-miR-328-3p	NRG2	hsa-miR-1180-3p	KIAA1324
hsa-miR-1180-3p	TNPO2	hsa-miR-328-3p	SPECC1L	hsa-miR-1180-3p	INTU
hsa-miR-1180-3p	TXNDC2	hsa-miR-328-3p	MPI	hsa-miR-1180-3p	WASF2
hsa-miR-1180-3p	CEP41	hsa-miR-328-3p	XKR7	hsa-miR-1180-3p	KBTBD11
hsa-miR-1180-3p	ATG9B	hsa-miR-328-3p	SORL1	hsa-miR-1180-3p	PRKCA
hsa-miR-1180-3p	CHCHD5	hsa-miR-328-3p	SHISA6	hsa-miR-1180-3p	ZNF710
hsa-miR-1180-3p	AC006486.1	hsa-miR-328-3p	TMEM64	hsa-miR-1180-3p	CLCN7
hsa-miR-1180-3p	EFCAB6	hsa-miR-328-3p	RAD23B	hsa-miR-1180-3p	TLE3
hsa-miR-1180-3p	IL25	hsa-miR-328-3p	WDTC1	hsa-miR-1180-3p	ZNF468
hsa-miR-1180-3p	CACNB2	hsa-miR-328-3p	GRM4	hsa-miR-1180-3p	IKZF5
hsa-miR-1180-3p	SNX21	hsa-miR-328-3p	PRDM16	hsa-miR-1180-3p	FAM211A
hsa-miR-1180-3p	TRAPPC3	hsa-miR-328-3p	C20orf112	hsa-miR-1180-3p	LMO4
hsa-miR-1180-3p	LRRC27	hsa-miR-328-3p	CPT1A	hsa-miR-1180-3p	MCC
hsa-miR-1180-3p	NYX	hsa-miR-328-3p	C1orf226	hsa-miR-1180-3p	AK2
hsa-miR-1180-3p	AC115618.1	hsa-miR-328-3p	ZNF618	hsa-miR-1180-3p	MTUS2
hsa-miR-1180-3p	FLJ14816	hsa-miR-328-3p	KIAA1549	hsa-miR-1180-3p	C1orf198
hsa-miR-1180-3p	NUDT16L1	hsa-miR-328-3p	IRAK1BP1	hsa-miR-1180-3p	SZT2
hsa-miR-1180-3p	APLP2	hsa-miR-328-3p	MN1	hsa-miR-1180-3p	SDAD1
hsa-miR-1180-3p	SLC32A1	hsa-miR-328-3p	PTPRF	hsa-miR-1180-3p	TNFRSF13C
hsa-miR-1180-3p	HIST1H2BD	hsa-miR-328-3p	SF1	hsa-miR-1180-3p	SPATA5
hsa-miR-1180-3p	STON1	hsa-miR-328-3p	RBM8A	hsa-miR-1180-3p	LSG1
hsa-miR-1180-3p	KLHDC4	hsa-miR-328-3p	PADI2	hsa-miR-1180-3p	FNBP1
hsa-miR-1180-3p	MLLT1	hsa-miR-328-3p	RP11-366L20.2	hsa-miR-1180-3p	IMPG2
hsa-miR-1180-3p	TMEM254	hsa-miR-328-3p	GSG1L	hsa-miR-1180-3p	CTIF
hsa-miR-1180-3p	XYLT1	hsa-miR-328-3p	MFSD2A	hsa-miR-1180-3p	LURAP1
hsa-miR-1180-3p	PIGS	hsa-miR-328-3p	ANKFY1	hsa-miR-1180-3p	SEC14L1
hsa-miR-1180-3p	FAM222B	hsa-miR-328-3p	SMC1A	hsa-miR-1180-3p	RPF2
hsa-miR-1180-3p	THBS2	hsa-miR-328-3p	HM13	hsa-miR-1180-3p	INF2
hsa-miR-1180-3p	KLHL36	hsa-miR-328-3p	CNIH4	hsa-miR-1180-3p	GOLT1B
hsa-miR-1180-3p	SAPCD2	hsa-miR-328-3p	ARPP19	hsa-miR-1180-3p	MYO9A
hsa-miR-1180-3p	CERS3	hsa-miR-328-3p	TSC1	hsa-miR-1180-3p	C19orf26
hsa-miR-1180-3p	HES2	hsa-miR-328-3p	TOM1	hsa-miR-1180-3p	RNF40
hsa-miR-1180-3p	TMEM88	hsa-miR-328-3p	ATPAF1	hsa-miR-1180-3p	LRCH4
hsa-miR-1180-3p	GINS4	hsa-miR-328-3p	MIB1	hsa-miR-1180-3p	ATXN3
hsa-miR-1180-3p	TTLL11	hsa-miR-328-3p	GRIN2B	hsa-miR-1180-3p	KCNV1
hsa-miR-1180-3p	AC129492.6	hsa-miR-328-3p	PLEKHA6	hsa-miR-1180-3p	KLF12
hsa-miR-1180-3p	BCL2L2-PABPN1	hsa-miR-328-3p	PTEN	hsa-miR-1180-3p	RXRA

Table 1 (continued)

miRNA	Target mRNA	miRNA	Target mRNA	miRNA	Target mRNA
hsa-miR-1180-3p	PCYT2	hsa-miR-328-3p	RPS3	hsa-miR-1180-3p	MRPS21
hsa-miR-1180-3p	SLC25A45	hsa-miR-328-3p	TOX4	hsa-miR-1180-3p	COL12A1
hsa-miR-1180-3p	ACKR2	hsa-miR-328-3p	C15orf37	hsa-miR-1180-3p	G3BP1
hsa-miR-1180-3p	FAM83F	hsa-miR-328-3p	DYNLL2	hsa-miR-1180-3p	ZNF609
hsa-miR-1180-3p	PPM1E	hsa-miR-328-3p	TMEM248	hsa-miR-1180-3p	HNRNPA2B1
hsa-miR-1180-3p	GJD3	hsa-miR-328-3p	NHSL2	hsa-miR-1180-3p	BMP8A
hsa-miR-1180-3p	TFEB	hsa-miR-328-3p	LEPROTL1	hsa-miR-1180-3p	ZNF555
hsa-miR-1180-3p	STIM1	hsa-miR-328-3p	ARHGEF17	hsa-miR-1180-3p	GPR180
hsa-miR-1180-3p	NELFB	hsa-miR-328-3p	RGP1	hsa-miR-1180-3p	LSM5
hsa-miR-1180-3p	BTD	hsa-miR-328-3p	LSM14B	hsa-miR-1180-3p	VIPR2
hsa-miR-1180-3p	ECE1	hsa-miR-328-3p	GOSR1	hsa-miR-1180-3p	SPRYD3
hsa-miR-1180-3p	EFNA2	hsa-miR-328-3p	SOX11	hsa-miR-1180-3p	GLG1
hsa-miR-1180-3p	YAP1	hsa-miR-328-3p	SLC8A1	hsa-miR-1180-3p	METTL20
hsa-miR-1180-3p	MTMR9	hsa-miR-328-3p	CREB1	hsa-miR-1180-3p	DUSP2
hsa-miR-1180-3p	WBSCR17	hsa-miR-328-3p	AGO1	hsa-miR-1180-3p	ARPC5L
hsa-miR-1180-3p	ZBTB38	hsa-miR-328-3p	ETV6	hsa-miR-1180-3p	MAPK1
hsa-miR-1180-3p	PABPN1	hsa-miR-328-3p	PPP2R5D	hsa-miR-1180-3p	C2orf48
hsa-miR-1180-3p	FAIM2	hsa-miR-328-3p	RAP1GAP2	hsa-miR-1180-3p	TOR4A
hsa-miR-1180-3p	TBC1D22A	hsa-miR-328-3p	ASIC1	hsa-miR-1180-3p	OARD1
hsa-miR-1180-3p	SLC25A34	hsa-miR-328-3p	CNOT2	hsa-miR-1180-3p	GGPS1
hsa-miR-1180-3p	ZNF837	hsa-miR-328-3p	EPB41L1	hsa-miR-1180-3p	CDH6
hsa-miR-1180-3p	QSOX2	hsa-miR-328-3p	CELSR2	hsa-miR-1180-3p	UCK2
hsa-miR-1180-3p	ENPP3	hsa-miR-328-3p	PPIP5K1	hsa-miR-1180-3p	CDCP1
hsa-miR-1180-3p	NFAM1	hsa-miR-328-3p	LMOD1	hsa-miR-1180-3p	C1orf95
hsa-miR-1180-3p	HAND2	hsa-miR-328-3p	GTDC1	hsa-miR-1180-3p	SH3BP2
hsa-miR-1180-3p	GRIK4	hsa-miR-328-3p	LPP	hsa-miR-1180-3p	HIST1H3B
hsa-miR-1180-3p	TTLL9	hsa-miR-328-3p	AP5M1	hsa-miR-1180-3p	RAPGEF1
hsa-miR-1180-3p	NDOR1	hsa-miR-328-3p	MECP2	hsa-miR-1180-3p	MBD5
hsa-miR-1180-3p	ARHGEF38	hsa-miR-328-3p	CTIF	hsa-miR-1180-3p	LINC00346
hsa-miR-1180-3p	CD53	hsa-miR-328-3p	ESRRA	hsa-miR-1180-3p	MRPS11
hsa-miR-1180-3p	SLC1A4	hsa-miR-328-3p	DNAJB14	hsa-miR-1180-3p	RBM7
hsa-miR-1180-3p	FXN	hsa-miR-328-3p	FGD1	hsa-miR-1180-3p	WNT9B
hsa-miR-1180-3p	KCNE4	hsa-miR-328-3p	FMNL3	hsa-miR-1180-3p	LHFPL4
hsa-miR-1180-3p	KRTAP5-10	hsa-miR-328-3p	SDK2	hsa-miR-1180-3p	SMURF1
hsa-miR-1180-3p	UQCRFS1	hsa-miR-328-3p	TMEM132B	hsa-miR-1180-3p	SLAIN2
hsa-miR-1180-3p	KCNMA1	hsa-miR-328-3p	LIMD1	hsa-miR-1180-3p	TIFAB
hsa-miR-1180-3p	AGK	hsa-miR-328-3p	RAB3C	hsa-miR-1180-3p	ADARB2
hsa-miR-1180-3p	AFF3	hsa-miR-328-3p	CBX8	hsa-miR-1180-3p	LRRC28
hsa-miR-1180-3p	SPSB1	hsa-miR-328-3p	PLA2G12A	hsa-miR-1180-3p	SP1
hsa-miR-1180-3p	MYO10	hsa-miR-328-3p	CTNS	hsa-miR-1180-3p	TXNDC17
hsa-miR-1180-3p	UBE2V1	hsa-miR-328-3p	GRAMD1B	hsa-miR-1180-3p	DUSP28
hsa-miR-1180-3p	HIST4H4	hsa-miR-328-3p	DNAJC18	hsa-miR-1180-3p	SEMA5A
hsa-miR-1180-3p	NRN1	hsa-miR-328-3p	NUFIP2	hsa-miR-1180-3p	ELFN2
hsa-miR-1180-3p	DDR1	hsa-miR-328-3p	RBP2	hsa-miR-1180-3p	DMD
hsa-miR-1180-3p	CTC-432M15.3	hsa-miR-328-3p	TGFB2	hsa-miR-1180-3p	ANKRD9
hsa-miR-1180-3p	CSF1	hsa-miR-328-3p	PLEKHG3	hsa-miR-1180-3p	RNF43
hsa-miR-1180-3p	SYNC	hsa-miR-328-3p	SIX1	hsa-miR-1180-3p	ANKMY1
hsa-miR-1180-3p	LRPAP1	hsa-miR-328-3p	NIT1	hsa-miR-1180-3p	HOXA3
hsa-miR-1180-3p	XPNPEP2	hsa-miR-328-3p	CACNG2	hsa-miR-1180-3p	FAM122A
hsa-miR-1180-3p	KIAA1644	hsa-miR-328-3p	HEYL	hsa-miR-1180-3p	FAM217B
hsa-miR-1180-3p	KRTAP5-11	hsa-miR-328-3p	FKBP15	hsa-miR-1180-3p	S1PR2
hsa-miR-1180-3p	MAP2K7	hsa-miR-328-3p	DRGX	hsa-miR-1180-3p	TCEA3
hsa-miR-1180-3p	GIT1	hsa-miR-1180-3p	EFHC1	hsa-miR-1180-3p	FANCA

Table 1 (continued)

miRNA	Target mRNA	miRNA	Target mRNA	miRNA	Target mRNA
hsa-miR-1180-3p	SLC6A1	hsa-miR-1180-3p	WIPF2	hsa-miR-1180-3p	ARSK
hsa-miR-1180-3p	HOXA10	hsa-miR-1180-3p	STARD10	hsa-miR-1180-3p	PMPCA
hsa-miR-1180-3p	RPS6KA1	hsa-miR-1180-3p	TNFAIP8	hsa-miR-1180-3p	CLYBL
hsa-miR-1180-3p	SYNDIG1	hsa-miR-1180-3p	GMPPB	hsa-miR-1180-3p	METTL21A
hsa-miR-1180-3p	RAPGEF6	hsa-miR-1180-3p	TRIM13	hsa-miR-1180-3p	CTC1
hsa-miR-1180-3p	NDRG1	hsa-miR-1180-3p	PCSK1	hsa-miR-1180-3p	TMED5
hsa-miR-1180-3p	PRRX2	hsa-miR-1180-3p	WDR76	hsa-miR-1180-3p	TTLL4
hsa-miR-1180-3p	VGF	hsa-miR-1180-3p	CELSR1	hsa-miR-1180-3p	RNF20
hsa-miR-1180-3p	ADAMTS1	hsa-miR-1180-3p	CCNL1	hsa-miR-1180-3p	C17orf51
hsa-miR-1180-3p	FAXDC2	hsa-miR-1180-3p	SLC45A4	hsa-miR-1180-3p	SELPLG
hsa-miR-1180-3p	ISOC2	hsa-miR-1180-3p	MYH9	hsa-miR-1180-3p	SPTB
hsa-miR-1180-3p	GPR157	hsa-miR-1180-3p	BRD3	hsa-miR-1180-3p	CA11
hsa-miR-1180-3p	HMG20B	hsa-miR-1180-3p	RAB3C	hsa-miR-1180-3p	SPN
hsa-miR-1180-3p	DKFZP761J1410	hsa-miR-1180-3p	MMADHC	hsa-miR-1180-3p	DYRK2
hsa-miR-1180-3p	C20orf197	hsa-miR-1180-3p	AIDA	hsa-miR-1180-3p	BMPR2
hsa-miR-1180-3p	RASA4B	hsa-miR-1180-3p	CENPM	hsa-miR-1180-3p	SLC30A10
hsa-miR-1180-3p	PCDH1	hsa-miR-1180-3p	SLC47A1	hsa-miR-1180-3p	SLFN12
hsa-miR-1180-3p	ATG4A	hsa-miR-1180-3p	HOXA13	hsa-miR-1180-3p	HECW2
hsa-miR-1180-3p	GGT6	hsa-miR-1180-3p	DBNL	hsa-miR-1180-3p	DST
hsa-miR-1180-3p	ZFP41	hsa-miR-1180-3p	RFC5	hsa-miR-1180-3p	ZMIZ1
hsa-miR-1180-3p	SDF4	hsa-miR-1180-3p	FDX1L	hsa-miR-1180-3p	SUMO2
hsa-miR-1180-3p	C17orf70	hsa-miR-1180-3p	BCAS3	hsa-miR-1180-3p	NOSIP
hsa-miR-1180-3p	C8orf46	hsa-miR-1180-3p	CSGALNACT2	hsa-miR-1180-3p	HMX1
hsa-miR-1180-3p	HIP1	hsa-miR-1180-3p	TAF3	hsa-miR-1180-3p	GIGYF2
hsa-miR-1180-3p	ZNF653	hsa-miR-1180-3p	CASK	hsa-miR-1180-3p	MGMT
hsa-miR-1180-3p	AMIGO3	hsa-miR-1180-3p	TAF6L	hsa-miR-1180-3p	ZNF177
hsa-miR-1180-3p	SP8	hsa-miR-1180-3p	RASAL2	hsa-miR-1180-3p	STX6
hsa-miR-1180-3p	WDR5	hsa-miR-1180-3p	C10orf32	hsa-miR-1180-3p	ZNF860
hsa-miR-1180-3p	GLYCTK	hsa-miR-1180-3p	WNK1	hsa-miR-1180-3p	MRPL23
hsa-miR-1180-3p	EIF4B	hsa-miR-1180-3p	TRDMT1	hsa-miR-1180-3p	RPAP2
hsa-miR-1180-3p	EVA1A	hsa-miR-1180-3p	RYBP	hsa-miR-1180-3p	AKT1
hsa-miR-1180-3p	SCMH1	hsa-miR-1180-3p	STRN	hsa-miR-1180-3p	METTL16
hsa-miR-1180-3p	SLC39A7	hsa-miR-1180-3p	ECHDC2	hsa-miR-1180-3p	EHBP1L1
hsa-miR-1180-3p	ZNF584	hsa-miR-1180-3p	MRTO4	hsa-miR-1180-3p	ARFRP1
hsa-miR-1180-3p	C5	hsa-miR-1180-3p	TTL	hsa-miR-1180-3p	IFRG15
hsa-miR-1180-3p	MLC1	hsa-miR-1180-3p	CYB5R1	hsa-miR-1180-3p	OTUB2
hsa-miR-1180-3p	LRIG1	hsa-miR-1180-3p	SUFU	hsa-miR-1180-3p	MSX2
hsa-miR-1180-3p	HSPBAP1	hsa-miR-1180-3p	TRIM11	hsa-miR-1180-3p	TACO1
hsa-miR-1180-3p	TBX2	hsa-miR-1180-3p	RRP8	hsa-miR-1180-3p	PAGR1
hsa-miR-1180-3p	DLX1	hsa-miR-1180-3p	GATA6	hsa-miR-1180-3p	LMF1
hsa-miR-1180-3p	AC026202.1	hsa-miR-1180-3p	CDKN2AIP	hsa-miR-1180-3p	TIFA
hsa-miR-1180-3p	ZNF534	hsa-miR-1180-3p	CHD9	hsa-miR-1180-3p	GNB1L
hsa-miR-1180-3p	ATP1A1	hsa-miR-1180-3p	HDAC2	hsa-miR-1180-3p	CITED2
hsa-miR-1180-3p	TMEM189	hsa-miR-1180-3p	CDR1as	hsa-miR-1180-3p	COX19
hsa-miR-1180-3p	TMEM189-UBE2V1	hsa-miR-1180-3p	TMEM134	hsa-miR-1180-3p	CEP63
hsa-miR-1180-3p	NID1	hsa-miR-1180-3p	COX6B1	hsa-miR-1180-3p	RP11-706O15.1
hsa-miR-1180-3p	RNF207	hsa-miR-1180-3p	GPRC5A	hsa-miR-1180-3p	SLCO1B3
hsa-miR-1180-3p	ELF5	hsa-miR-1180-3p	ACTRT2	hsa-miR-1180-3p	MTHFD1
hsa-miR-1180-3p	DNAJC22	hsa-miR-1180-3p	CACNG2	hsa-miR-1180-3p	CDX2
hsa-miR-1180-3p	WDR5B	hsa-miR-1180-3p	URB1	hsa-miR-1180-3p	TRAF1
hsa-miR-1180-3p	PRR23A	hsa-miR-1180-3p	SRCAP	hsa-miR-1180-3p	PPIL4
hsa-miR-1180-3p	CAMKK2	hsa-miR-1180-3p	CXorf40A	hsa-miR-1180-3p	HMGCR
hsa-miR-1180-3p	DOCK3	hsa-miR-1180-3p	LAMA4	hsa-miR-1180-3p	ABCC11

Table 1 (continued)

miRNA	Target mRNA	miRNA	Target mRNA	miRNA	Target mRNA
hsa-miR-1180-3p	C9orf170	hsa-miR-1180-3p	YAE1D1	hsa-miR-1180-3p	C17orf72
hsa-miR-1180-3p	GBGT1	hsa-miR-1180-3p	FECH	hsa-miR-1180-3p	TSC22D2
hsa-miR-1180-3p	MFAP1	hsa-miR-1180-3p	C11orf54	hsa-miR-1180-3p	GTF2B
hsa-miR-1180-3p	TSPAN14	hsa-miR-1180-3p	GRIN2A	hsa-miR-1180-3p	ATG2A
hsa-miR-1180-3p	ACTRT3	hsa-miR-1180-3p	PIM3	hsa-miR-1180-3p	SOX14
hsa-miR-1180-3p	SLIT3	hsa-miR-1180-3p	ZNF426	hsa-miR-1180-3p	SBF1
hsa-miR-1180-3p	P2RX5	hsa-miR-1180-3p	CNDP2	hsa-miR-1180-3p	USPL1
hsa-miR-1180-3p	CDK5R2	hsa-miR-1180-3p	NRBF2	hsa-miR-1180-3p	SPATS2L
hsa-miR-1180-3p	TBX15	hsa-miR-1180-3p	HECTD3	hsa-miR-1180-3p	ANGPT4
hsa-miR-1180-3p	IER5	hsa-miR-1180-3p	LDOC1L	hsa-miR-1180-3p	VCAN
hsa-miR-1180-3p	FRAT1	hsa-miR-1180-3p	RAB6A	hsa-miR-1180-3p	GATSL2
hsa-miR-1180-3p	RAB15	hsa-miR-1180-3p	EMR2	hsa-miR-1180-3p	HOXB2
hsa-miR-1180-3p	UTP15	hsa-miR-1180-3p	LOH12CR1	hsa-miR-1180-3p	SF3B5
hsa-miR-1180-3p	TBCE	hsa-miR-1180-3p	C20orf194	hsa-miR-1180-3p	PNRC1
hsa-miR-1180-3p	UBR7	hsa-miR-1180-3p	DCAF4L2	hsa-miR-1180-3p	ATP12A
hsa-miR-1180-3p	NRXN2	hsa-miR-1180-3p	C1orf200	hsa-miR-1180-3p	AKR7A2
hsa-miR-1180-3p	RIMS1	hsa-miR-1180-3p	WNK2	hsa-miR-1180-3p	ZNF703
hsa-miR-1180-3p	ZNF821	hsa-miR-1180-3p	C6orf222	hsa-miR-1180-3p	CADM1
hsa-miR-1180-3p	EMB	hsa-miR-1180-3p	CAPN6	hsa-miR-1180-3p	ZNHIT1
hsa-miR-1180-3p	NCOA4	hsa-miR-1180-3p	PITPNC1	hsa-miR-1180-3p	CD72
hsa-miR-1180-3p	CIITA	hsa-miR-1180-3p	CAMSAP1	hsa-miR-1180-3p	DNAJB4
hsa-miR-1180-3p	PINK1	hsa-miR-1180-3p	FOXN3	hsa-miR-1180-3p	FBXO31
hsa-miR-1180-3p	TACSTD2	hsa-miR-1180-3p	COL1A1	hsa-miR-1180-3p	PTAFR
hsa-miR-1180-3p	EYA1	hsa-miR-1180-3p	ITIH6	hsa-miR-1180-3p	FAM90A26
hsa-miR-1180-3p	OLIG1	hsa-miR-1180-3p	KLLN	hsa-miR-1180-3p	CPD
hsa-miR-1180-3p	MPRIP	hsa-miR-1180-3p	RER1	hsa-miR-1180-3p	TGFB1I1
hsa-miR-1180-3p	TRAPPC11	hsa-miR-1180-3p	SNAPC5	hsa-miR-1180-3p	ELMSAN1
hsa-miR-1180-3p	POTEI	hsa-miR-1180-3p	C11orf52	hsa-miR-1180-3p	C15orf53
hsa-miR-1180-3p	PITPNA	hsa-miR-1180-3p	AL354898.1	hsa-miR-1180-3p	C17orf107
hsa-miR-1180-3p	CNPY1	hsa-miR-1180-3p	GLI4	hsa-miR-1180-3p	CCDC140
hsa-miR-1180-3p	GREM2	hsa-miR-1180-3p	SLC6A20	hsa-miR-1180-3p	MYADML2
hsa-miR-1180-3p	CDIP1	hsa-miR-1180-3p	TMEM255A	hsa-miR-1180-3p	MBNL1
hsa-miR-1180-3p	SPRY4	hsa-miR-1180-3p	CENPO	hsa-miR-1180-3p	FGFR3
hsa-miR-1180-3p	MOB3A	hsa-miR-1180-3p	DOK4	hsa-miR-1180-3p	TRIM24
hsa-miR-1180-3p	C8orf82	hsa-miR-1180-3p	ACSS2	hsa-miR-1180-3p	POMGNT1
hsa-miR-1180-3p	SP9	hsa-miR-1180-3p	CCDC64	hsa-miR-1180-3p	DNAJC6
hsa-miR-1180-3p	RANBP10	hsa-miR-1180-3p	RAPGEF2	hsa-miR-1180-3p	DRAXIN
hsa-miR-1180-3p	GRM1	hsa-miR-1180-3p	ZNF317	hsa-miR-1180-3p	RALGPS1
hsa-miR-1180-3p	TMCO4	hsa-miR-1180-3p	CYP26B1	hsa-miR-1180-3p	TPH2
hsa-miR-1180-3p	TIRAP	hsa-miR-1180-3p	RAB6C		

miRNAs in SBNETs related signaling pathways. Through drug target prediction, the key genes and their relationships with the immune environment were further identified.

Identifying novel biomarkers in SBNETs has proven challenging. The development of next-generation sequencing has allowed researchers to objectively explore tumor specimens and understand the molecular landscape involved in the malignant transformation of SBNETs. It has recently been shown that miRNAs are involved in the metastasis of SBNETs [21], and altered expression of miRNAs specifically in SBNETs could provide actionable therapeutic targets [30]. Among the feature miRNAs we identified, a negative correlation between miR – 375 and Yap appears to be required for the differentiation and proliferation of neuroendocrine lung xenografts [31]. Based on the current tissue Atlas

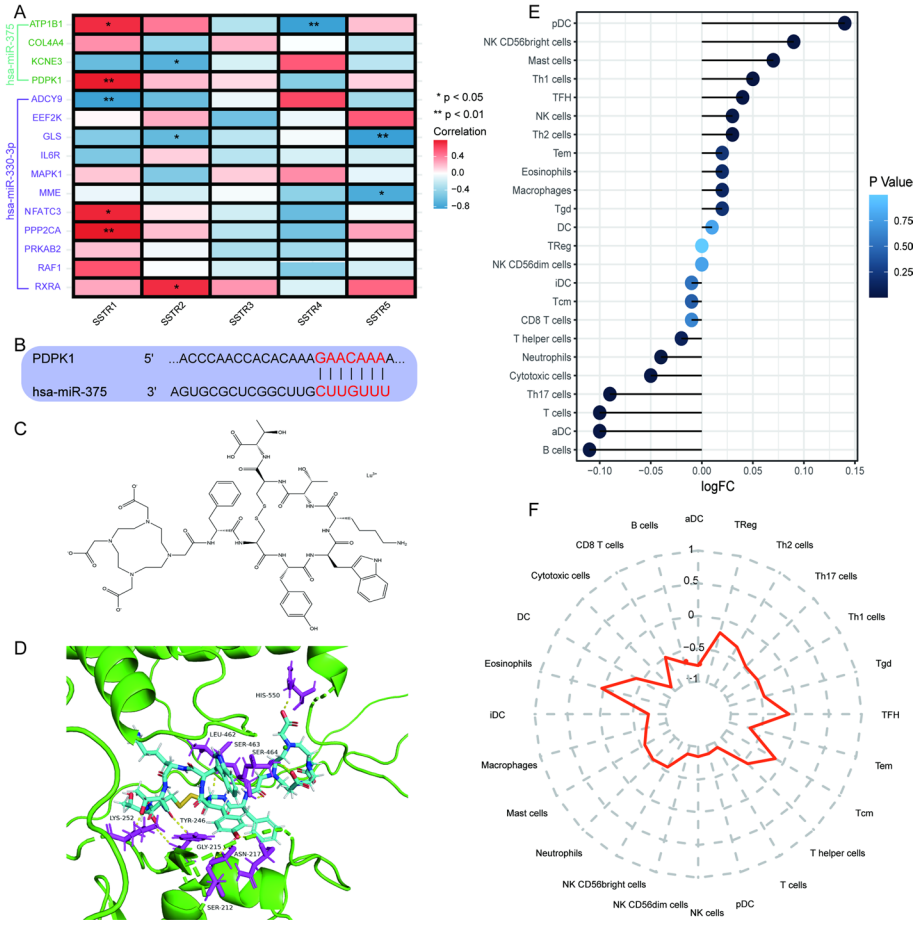

Fig. 6 Target-drug interactions and immune evaluation. **A** Correlation between target genes of feature miRNAs and target genes of 177Lu-DOTATATE. **B** Binding sites between PDPK1 and miR−375 predicted by Targetscan database. **C** Structural formula of 177Lu-DOTATATE. **D** The active site of SSTR1 docking to 177Lu-DOTATATE. **E** Differential levels of immune cells between SBNET and control. **F** Correlations between immune cells and PDPK1

of miRNAs expression, miR−375 is currently considered as an endocrine gland specific marker [32]. MiR−375 is a universal marker of neuroendocrine cell differentiation, and its expression is proportional to the degree of neuroendocrine differentiation in tumors [33]. MiR−107 is upregulated in SBNETs [34] and can significantly distinguish cancer and non-cancer tissues [35]. MiR−1180 can accelerate cell proliferation in ovarian cancer, hepatocellular carcinoma, lung cancer [36–38]. MiR−1180 is an independent predictor of survival in pancreatic cancer patients [39]. MiR−330−3p was found to be a gene with SBNETs specific untranslated regions polyadenylation [40]. MiR−330−3p has diagnostic and prognostic potential in prostate cancer [41]. Overexpression of MiR−330−3p promotes liver cancer progression by enhancing tumor cell invasiveness through epithelial mesenchymal transition activation [42]. MiR−328 in the pancreas has been identified as a biomarker for gastroenteropancreatic NETs [43].

Furthermore, miR-107 is known to target CDK6, which primarily influence proliferation in colorectal cancer [44]. MiR-1180 has been reported to suppress TNIP2 that pro-proliferative effects in hepatocellular cancers likely operate through apoptosis evasion rather than neuroendocrine-specific pathways [37]. miR-328 targets ABCG2 that down-regulation of miR-328 inhibits the proliferation, invasion and migration of gastric cancer

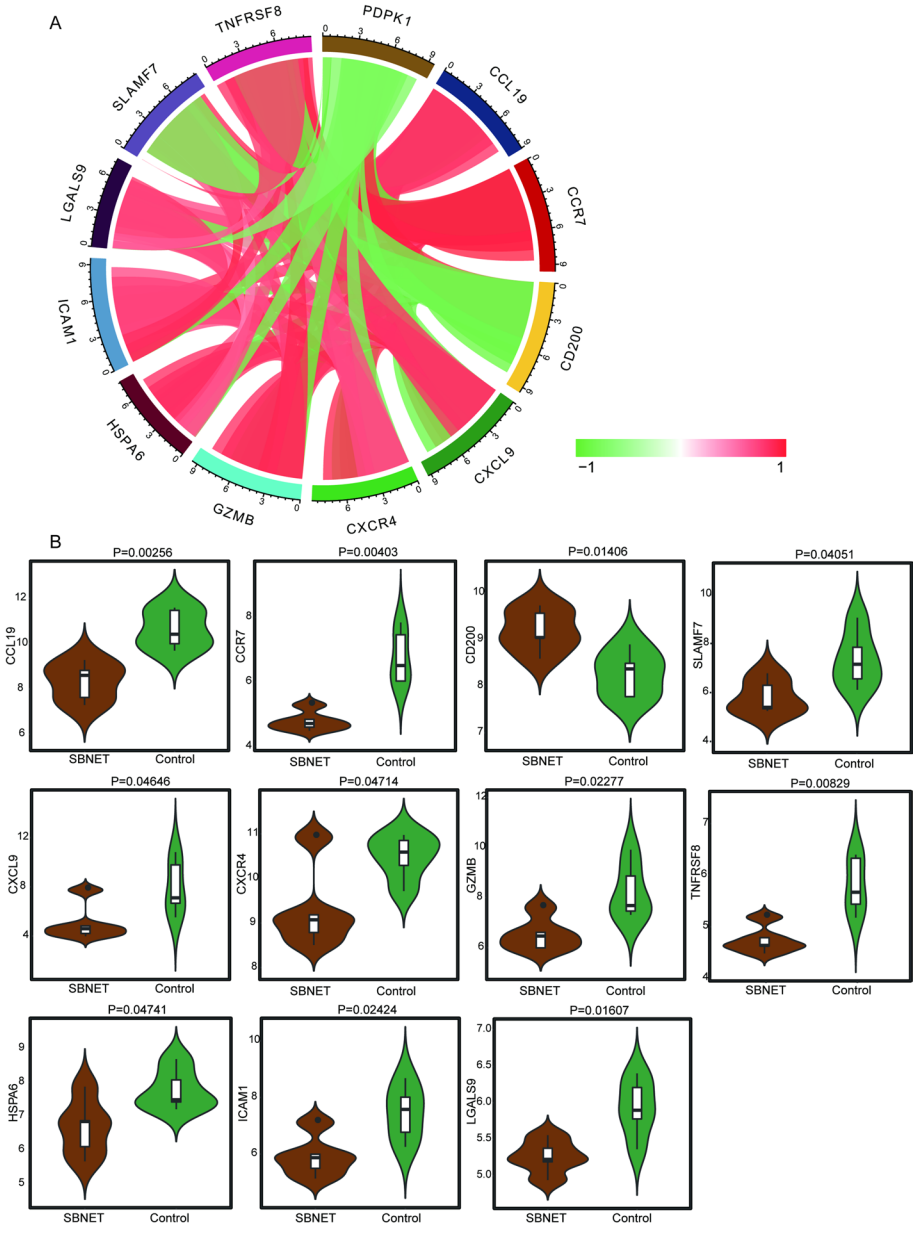

Fig. 7 Immune checkpoints and PDPK1. (**A**) Correlations between immune checkpoints and PDPK1. (**B**) Differential levels of checkpoints between SBNET and control

cell lines [45], suggesting roles in metastasis that may be context-dependent in SBNETs. Above all, future studies combining miRNA-mRNA co-expression analysis with functional validation in SBNET models will help clarify these relationships.

On the other hand, we identified the biological roles in which DEmRs were involved. AMPK signaling, which is activated under conditions of glucose deprivation, heat shock, oxidative stress, and ischemia, is a key component of protection against various inflammatory signals [46]. NETs involve both AMPK dependent and AMPK independent pathways [47]. PPARs are fatty acid activated transcription factors in the nuclear hormone receptor superfamily that regulate energy metabolism [48]. As multifunctional molecules, PPARs have been implicated in a variety of human diseases such as cancer, metabolic and autoimmune diseases [49–51].

Recent studies have also shown that Th17 cells enhance antitumor immunity by directly promoting the proliferation of cytotoxic T lymphocytes [52]. In peripheral and tissue infiltrating Th17 cells of melanoma patients, the anti-apoptotic protein Bcl-2 is downregulated, while the pro apoptotic protein activated caspase-3 is upregulated [53]. GnRH antagonists / agonists have emerged as one of the treatments for metastatic prostate cancer [54]. Although limited studies confirm, our results show that these signaling pathways may be involved in SBNETs.

Based on the results of three phase clinical trials that early intervention with 177Lu-DOTATATE improves outcomes in pancreatic NETs [55]. We predicted the discovery of 177Lu-DOTATATE as a targeted therapeutic agent for SBNETs. Importantly, through drug prediction we identified that PDPK1 might be significantly associated with drug targets and regulated by miR – 375. PDPK1 expression is significantly higher in small cell lung cancer tissues and correlates with patient characteristics [56]. PDPK1 promotes Akt activation and contributes to PTEN-null-associated prostate cancer progression through a positive feedback loop [57]. PDPK1 small molecule inhibition increases medulloblastoma survival and enhances the cytotoxic effects of chemotherapeutic agents [58]. PDPK1 is an emerging cancer stem cell target in some cancer histologies [56]. Loss of PDPK1 enhances immunostimulatory efficacy in melanoma [59]. Although no other studies to date have demonstrated a direct link of PDPK1 to SBNETs, our results suggest that it may be a potential therapeutic marker.

We further found a negative correlation between PDPK1 and lowly infiltrated immune cells in SBNETs, especially cytotoxic cells. This observation suggests that PDPK1 may contribute to an immunosuppressive tumor microenvironment by inhibiting cytotoxic immune cell infiltration. Notably, several miRNAs were also correlated with immune checkpoint molecules, raising the possibility that miRNA-mediated regulation of immune checkpoints could modulate anti-tumor immunity in SBNETs. The miR-107-3p suppresses PD-L1 in hepatocellular carcinoma, thereby enhancing the anticancer immune response [60]. miR-375 was negatively correlated with PD-L1 in gastric cancer that could be a promising novel therapeutic target in gastric cancer [61]. These findings highlight the potential of miRNAs as therapeutic targets to reverse immune evasion in SBNETs. In addition, CD200 is a relatively sensitive marker for nets, which is associated with tumor grade and may serve as a potential therapeutic target [62, 63]. CCR7 was shown to be required for the ability of dendritic cells to metastasize from the tumor to draining lymph nodes and subsequently activate T cells [64]. This implies that PDPK1 may also be associated with immunosuppression in SBNETs and in turn be involved in the progression of the disease. However, the immune landscape of SBNETs remains undercharacterized, particularly regarding the roles of immune checkpoints and infiltrating immune cells. Therefore, combining immune checkpoint inhibitors with miRNA-based therapies may enhance treatment efficacy by simultaneously blocking immune evasion and promoting cytotoxic immune cell infiltration, offering a promising strategy to restore anti-tumor immunity.

There are limitations to the present study. This is a data collection from public database with less sample specific clinical information, making generalizability limited. The key results need to be deeply investigated utilizing in vivo and in vitro experiments. While our study identified a set of miRNAs with diagnostic potential and explored their biological roles, the correlation with prognosis was not extensively investigated due to

the lack of comprehensive clinical follow-up data in the available datasets. Future studies should aim to integrate miRNA expression profiles with long-term clinical outcomes to evaluate the prognostic value of these miRNAs in SBNET. Additionally, functional studies are needed to elucidate the mechanisms by which these miRNAs influence disease progression and patient survival. The current study did not have enough data for adjuvant therapy, which may affect the limitations of the application of miRNA regulatory networks as therapeutic and prognostic.

5 Conclusion

This study explored the potential diagnostic roles of miRNAs, as well as the downstream regulatory networks and molecular mechanisms. Regulation of PDPK1 by miR – 375 may provide a useful basis for the design of therapeutic agents for SBNETs in the future.

Acknowledgements
Not applicable.

Author contributions
TR conceived the study and drafted the manuscript. LZ and ZLL performed bioinformatic and statistical analysis. MMP downloaded and collated the data in the article. XQH critically reviewed the manuscript. All authors read and approved the final manuscript.

Funding
This work was supported by the Guangxi Health Commission self-funded research project, METTL1 mediates non-small cell lung cancer resistance to immunotherapy by stimulating macrophage M2 polarisation (Z-A20231129).

Declarations
Competing Interests.
The authors have no relevant financial or non-financial interests to disclose.

Data availability
The datasets analysed during the current study are available in the gene expression omnibus (GEO) repository, [https://www.ncbi.nlm.nih.gov/].

Received: 27 November 2024 / Accepted: 30 May 2025
Published online: 23 June 2025

References

1. Herrera-Martinez AD, Hofland J, Hofland LJ, Brabander T, Eskens F, Galvez Moreno MA, Luque RM, Castano JP, de Herder WW, Feelders RA. Targeted systemic treatment of neuroendocrine tumors: current options and future perspectives. Drugs. 2019;79(1):21–42.
2. Kunz PL. Carcinoid and neuroendocrine tumors: Building on success. J Clin Oncol. 2015;33(16):1855–63.
3. Tran CG, Sherman SK, Howe JR. The landmark series: management of small bowel neuroendocrine tumors. Ann Surg Oncol. 2021;28(5):2741–51.
4. Tran CG, Sherman SK, Howe JR. Small bowel neuroendocrine tumors. Curr Probl Surg. 2020;57(12):100823.
5. Di Domenico A, Wiedmer T, Marinoni I, Perren A. Genetic and epigenetic drivers of neuroendocrine tumours (NET). Endocr Relat Cancer. 2017;24(9):R315–34.
6. Kacmaz E, Sarasqueta AF, van Eeden S, Dreijerink KMA, Klumpen HJ, Tanis PJ, van Dijkum E, Engelsman AF. Update on incidence, prevalence, treatment and survival of patients with small bowel neuroendocrine neoplasms in the Netherlands. World J Surg. 2021;45(8):2482–91.
7. Dasari A, Shen C, Halperin D, Zhao B, Zhou S, Xu Y, Shih T, Yao JC. Trends in the incidence, prevalence, and survival outcomes in patients with neuroendocrine tumors in the united States. JAMA Oncol. 2017;3(10):1335–42.
8. Kacmaz E, Chen JW, Tanis PJ, van Nieveen EJM, Engelsman AF. Postoperative morbidity and mortality after surgical resection of small bowel neuroendocrine neoplasms: A systematic review and meta-analysis. J Neuroendocrinol. 2021;33(8):e13008.
9. Maxwell JE, Sherman SK, O'Dorisio TM, Bellizzi AM, Howe JR. Liver-directed surgery of neuroendocrine metastases: what is the optimal strategy? Surgery. 2016;159(1):320–33.
10. Heublein S, Albertsmeier M, Pfeifer D, Loehrs L, Bazhin AV, Kirchner T, Werner J, Neumann J, Angele MK. Association of differential MiRNA expression with hepatic vs. peritoneal metastatic spread in colorectal cancer. BMC Cancer. 2018;18(1):201.
11. Zhang X, Zhang D, Bu X, Zhang X, Cui L. Identification of a novel miRNA-based recurrence and prognosis prediction biomarker for hepatocellular carcinoma. BMC Bioinformatics. 2022;23(1):479.
12. Md Zaki FA, Mohamad Hanif EA. Identifying MiRNA as biomarker for breast cancer subtyping using association rule. Comput Biol Med. 2024;178:108696.
13. Bosch F, Bazhin AV, Heublein S, Bruwer K, Knosel T, Reiter FP, Auernhammer CJ, Guba MO, Spitzweg C, Werner J, et al. Treatment with somatostatin analogs induces differentially expressed let-7c-5p and mir-3137 in small intestine neuroendocrine tumors. BMC Cancer. 2019;19(1):575.

14. Bongiovanni A, Liverani C, Foca F, Bergamo F, Leo S, Pusceddu S, Gelsomino F, Brizzi MP, Di Meglio G, Spada F, et al. A randomized phase II trial of Captem or Folfiri as second-line therapy in neuroendocrine carcinomas. Eur J Cancer. 2024;208:114129.
15. Shorning BY, Dass MS, Smalley MJ, Pearson HB. The PI3K-AKT-mTOR pathway and prostate cancer: at the crossroads of AR, MAPK, and WNT signaling. Int J Mol Sci 2020, 21(12).
16. Nalairndran G, Hassan Abdul Razack A, Mai CW, Fei-Lei Chung F, Chan KK, Hii LW, Lim WM, Chung I, Leong CO. Phosphoinositide-dependent kinase-1 (PDPK1) regulates serum/glucocorticoid-regulated kinase 3 (SGK3) for prostate cancer cell survival. J Cell Mol Med. 2020;24(20):12188–98.
17. Mihaly Z, Kormos M, Lanczky A, Dank M, Budczies J, Szasz MA, Gyorffy B. A meta-analysis of gene expression-based biomarkers predicting outcome after Tamoxifen treatment in breast cancer. Breast Cancer Res Treat. 2013;140(2):219–32.
18. Bai X, Li P, Xie Y, Guo C, Sun Y, Xu Q, Zhao D. Overexpression of 3-phosphoinositide-dependent protein kinase-1 is associated with prognosis of gastric carcinoma. Tumour Biol. 2016;37(2):2333–9.
19. Wang J, Liu F, Ao P, Li X, Zheng H, Wu D, Zhang N, She J, Yuan J, Wu X. Correlation of PDK1 expression with clinicopathologic features and prognosis of hepatocellular carcinoma. Onco Targets Ther. 2016;9:5597–602.
20. Dang Y, Chen J, Feng W, Qiao C, Han W, Nie Y, Wu K, Fan D, Xia L. Interleukin 1beta-mediated HOXC10 overexpression promotes hepatocellular carcinoma metastasis by upregulating PDPK1 and VASP. Theranostics. 2020;10(8):3833–48.
21. Miller HC, Frampton AE, Malczewska A, Ottaviani S, Stronach EA, Flora R, Kaemmerer D, Schwach G, Pfragner R, Faiz O, et al. MicroRNAs associated with small bowel neuroendocrine tumours and their metastases. Endocr Relat Cancer. 2016;23(9):711–26.
22. Andersson E, Arvidsson Y, Sward C, Hofving T, Wangberg B, Kristiansson E, Nilsson O. Expression profiling of small intestinal neuroendocrine tumors identifies subgroups with clinical relevance, prognostic markers and therapeutic targets. Mod Pathol. 2016;29(6):616–29.
23. Ritchie ME, Phipson B, Wu D, Hu Y, Law CW, Shi W, Smyth GK. Limma powers differential expression analyses for RNA-sequencing and microarray studies. Nucleic Acids Res. 2015;43(7):e47.
24. Yu G, Wang LG, Han Y, He QY. ClusterProfiler: an R package for comparing biological themes among gene clusters. OMICS. 2012;16(5):284–7.
25. Liang H, Jiang K, Yan TA, Chen GH. XGBoost: an optimal machine learning model with just structural features to discover MOF adsorbents of xe/kr. ACS Omega. 2021;6(13):9066–76.
26. Smith M, Alvarez F. Identifying mortality factors from machine learning using Shapley values - a case of COVID19. Expert Syst Appl. 2021;176:114832.
27. Langfelder P, Horvath S. WGCNA: an R package for weighted correlation network analysis. BMC Bioinformatics. 2008;9:559.
28. Salmena L, Poliseno L, Tay Y, Kats L, Pandolfi PP. A CeRNA hypothesis: the Rosetta stone of a hidden RNA language? Cell. 2011;146(3):353–8.
29. Hanzelmann S, Castelo R, Guinney J. GSVA: gene set variation analysis for microarray and RNA-seq data. BMC Bioinformatics. 2013;14:7.
30. Samsom KG, van Veenendaal LM, Valk GD, Vriens MR, Tesselaar MET, van den Berg JG. Molecular prognostic factors in small-intestinal neuroendocrine tumours. Endocr Connect. 2019;8(7):906–22.
31. Yang X, Nanayakkara J, Claypool D, Saghafinia S, Wong JJM, Xu M, Wang X, Nicol CJB, Michael IP, Hafner M, et al. A miR-375/YAP axis regulates neuroendocrine differentiation and tumorigenesis in lung carcinoid cells. Sci Rep. 2021;11(1):10455.
32. Ludwig N, Leidinger P, Becker K, Backes C, Fehlmann T, Pallasch C, Rheinheimer S, Meder B, Stahler C, Meese E, et al. Distribution of MiRNA expression across human tissues. Nucleic Acids Res. 2016;44(8):3865–77.
33. Nanayakkara J, Tyryshkin K, Yang X, Wong JJM, Vanderbeck K, Ginter PS, Scognamiglio T, Chen YT, Panarelli N, Cheung NK, et al. Characterizing and classifying neuroendocrine neoplasms through MicroRNA sequencing and data mining. NAR Cancer. 2020;2(3):zcaa009.
34. Roldo C, Missiaglia E, Hagan JP, Falconi M, Capelli P, Bersani S, Calin GA, Volinia S, Liu CG, Scarpa A, et al. MicroRNA expression abnormalities in pancreatic endocrine and acinar tumors are associated with distinctive pathologic features and clinical behavior. J Clin Oncol. 2006;24(29):4677–84.
35. Mafficini A, Scarpa A. Genetics and epigenetics of gastroenteropancreatic neuroendocrine neoplasms. Endocr Rev. 2019;40(2):506–36.
36. Hu J, Zhao W, Huang Y, Wang Z, Jiang T, Wang L. MiR-1180 from bone marrow MSCs promotes cell proliferation and Glycolysis in ovarian cancer cells via SFRP1/Wnt pathway. Cancer Cell Int. 2019;19:66.
37. Zhou X, Zhu HQ, Ma CQ, Li HG, Liu FF, Chang H, Lu J. MiR-1180 promoted the proliferation of hepatocellular carcinoma cells by repressing TNIP2 expression. Biomed Pharmacother. 2016;79:315–20.
38. Chen EG, Zhang JS, Xu S, Zhu XJ, Hu HH. Long non-coding RNA DGCR5 is involved in the regulation of proliferation, migration and invasion of lung cancer by targeting miR-1180. Am J Cancer Res. 2017;7(7):1463–75.
39. Dou D, Yang S, Lin Y, Zhang J. An eight-miRNA signature expression-based risk scoring system for prediction of survival in pancreatic adenocarcinoma. Cancer Biomark. 2018;23(1):79–93.
40. Rehfeld A, Plass M, Dossing K, Knigge U, Kjaer A, Krogh A, Friis-Hansen L. Alternative polyadenylation of tumor suppressor genes in small intestinal neuroendocrine tumors. Front Endocrinol (Lausanne). 2014;5:46.
41. Arrighetti N, Beretta GL. MiRNAs as therapeutic tools and biomarkers for prostate Cancer. Pharmaceutics 2021, 13(3).
42. Yang S, Zhang Y, Guo C, Liu R, Elkharti M, Ge Z, Liu Q, Liu S, Sun MZ. The homeostatic malfunction of a novel feedback pathway formed by lncRNA021545, miR-330-3p and Epiregulin contributes in hepatocarcinoma progression via mediating epithelial-mesenchymal transition. Am J Cancer Res. 2022;12(6):2492–525.
43. Fang JM, Li J, Shi J. An update on the diagnosis of gastroenteropancreatic neuroendocrine neoplasms. World J Gastroenterol. 2022;28(10):1009–23.
44. Li D, Peng M, Zhou J. Noncoding RNA Linc00475 promotes the proliferation of colorectal cancer cells by targeting miR-107/CDK6 axis. J Biochem Mol Toxicol. 2024;38(11):e70012.
45. Yan BL, Li XL, An JY. MicroRNA-328 acts as an anti-oncogene by targeting ABCG2 in gastric carcinoma. Eur Rev Med Pharmacol Sci. 2019;23(14):6148–59.
46. Noor HB, Mou NA, Salem L, Shimul MFA, Biswas S, Akther R, Khan S, Raihan S, Mohib MM, Sagor MAT. Anti-inflammatory property of AMP-activated protein kinase. Antiinflamm Antiallergy Agents Med Chem. 2020;19(1):2–41.

47. Vlotides G, Tanyeri A, Spampatti M, Zitzmann K, Chourdakis M, Sptti C, Maurer J, Nolting S, Goke B, Auernhammer CJ. Anticancer effects of Metformin on neuroendocrine tumor cells in vitro. Horm (Athens). 2014;13(4):498–508.
48. Christofides A, Konstantinidou E, Jani C, Boussiotis VA. The role of peroxisome proliferator-activated receptors (PPAR) in immune responses. Metabolism. 2021;114:154338.
49. Wagner N, Wagner KD. Peroxisome Proliferator-Activated receptors and the hallmarks of Cancer. Cells 2022, 11(15).
50. Wang Y, Nakajima T, Gonzalez FJ, Tanaka N. PPARs as metabolic regulators in the liver: lessons from Liver-Specific PPAR-Null mice. Int J Mol Sci 2020, 21(6).
51. Stark JM, Coquet JM, Tibbitt CA. The role of PPAR-gamma in allergic disease. Curr Allergy Asthma Rep. 2021;21(11):45.
52. Yamamoto S, Matsuo K, Sakai S, Mishima I, Hara Y, Oiso N, Kawada A, Yoshie O, Nakayama T. P2X receptor agonist enhances tumor-specific CTL responses through CD70 + DC-mediated Th17 induction. Int Immunol. 2021;33(1):49–55.
53. He H, Qiao B, Guo S, Cui H, Li N, Liu H, Qin J, He J, Yang X, Xue W, et al. Induction of T helper 17 cell response by interleukin-7 in patients with primary cutaneous melanoma. Melanoma Res. 2021;31(4):328–37.
54. He Y, Xu W, Xiao YT, Huang H, Gu D, Ren S. Targeting signaling pathways in prostate cancer: mechanisms and clinical trials. Signal Transduct Target Ther. 2022;7(1):198.
55. Fross-Baron K, Garske-Roman U, Welin S, Granberg D, Eriksson B, Khan T, Sandstrom M, Sundin A. 177Lu-DOTATATE therapy of advanced pancreatic neuroendocrine tumors heavily pretreated with chemotherapy: analysis of outcome, safety, and their determinants. Neuroendocrinology. 2021;111(4):330–43.
56. Domrachev B, Singh S, Li D, Rudloff U. Mini-Review: PDPK1 (3-phosphoinositide dependent protein kinase-1), an emerging Cancer stem cell target. J Cancer Treat Diagn. 2021;5(1):30–5.
57. Ding Y, Chi H, Shao J, Shi T, Yu H, Wang X, Wang X. Leukemia inhibitory factor receptor homodimerization mediated by acetylation of extracellular lysine promotes prostate cancer progression through the PDPK1/AKT/GCN5 axis. Clin Transl Med. 2022;12(2):e676.
58. Baryawno N, Sveinbjornsson B, Eksborg S, Chen CS, Kogner P, Johnsen JI. Small-molecule inhibitors of phosphatidylinositol 3-kinase/Akt signaling inhibit Wnt/beta-catenin pathway cross-talk and suppress Medulloblastoma growth. Cancer Res. 2010;70(1):266–76.
59. Cai W, Nguyen MQ, Wilski NA, Purwin TJ, Vernon M, Tiago M, Aplin AE. A Genome-Wide screen identifies PDPK1 as a target to enhance the efficacy of MEK1/2 inhibitors in NRAS mutant melanoma. Cancer Res. 2022;82(14):2625–39.
60. Zhang C, Chen Y, Han J, Liu R, Liu C, Zhao Y, Liu Y. Ultrasound nanobubble-based combinational strategies of loaded miR-107-3p and CD133 Ab for anti-PD-L1 and anti-hepatocellular cancer stem cells. Int J Pharm. 2025;670:125140.
61. Yan XL, Luo QY, Zhou SN, Pan WT, Zhang L, Yang DJ, Qiu MZ. MicroRNA-375 reverses the expression of PD-L1 by inactivating the JAK2/STAT3 signaling pathways in gastric cancer. Clin Res Hepatol Gastroenterol. 2021;45(5):101574.
62. Cao Z, Cen HB, Wei JG, Qin LZ, Liao W, Ao QL. [Expression of CD200 and INSM1 in Gastrointestinal and pancreatic neuroendocrine neoplasms and its diagnostic values]. Zhonghua Bing Li Xue Za Zhi. 2021;50(10):1134–8.
63. Love JE, Thompson K, Kilgore MR, Westerhoff M, Murphy CE, Papanicolau-Sengos A, McCormick KA, Shankaran V, Vandeven N, Miller F, et al. CD200 expression in neuroendocrine neoplasms. Am J Clin Pathol. 2017;148(3):236–42.
64. Roberts EW, Broz ML, Binnewies M, Headley MB, Nelson AE, Wolf DM, Kaisho T, Bogunovic D, Bhardwaj N, Krummel MF. Critical role for CD103(+)/CD141(+) dendritic cells bearing CCR7 for tumor antigen trafficking and priming of T cell immunity in melanoma. Cancer Cell. 2016;30(2):324–36.

Publisher's note